

Quasi-Hermitian extended SSH models

Iao-Fai Io^{a,1}, Cheng-Yuan Huang^{b,1}, Jhih-Shih You^{c,2}, Hao-Chun Chang^{d,3} and Hsien-chung Kao^{e,2}

¹Physics Department, National Taiwan University, Taipei 10617, Taiwan

²Physics Department, National Taiwan Normal University, Taipei 11677, Taiwan

³Electrophysics Department, National Yang Ming Chiao Tung University, Hsinchu 30050, Taiwan

(Dated: August 22, 2023)

We consider the quasi-Hermitian limit of a non-Hermitian extended Su–Schrieffer–Heeger model, in which the hopping amplitudes obey a specific relation so that the system may be mapped to a corresponding Hermitian one and its energy spectrum is completely real. Analogous to the Hermitian case, one may use the modified winding number $\bar{\nu}$ to determine the total number of edge states on the boundaries so that a modified bulk–boundary correspondence may be achieved. Due to the skin effect in non-Hermitian systems, the spectral winding numbers ν_E^L and ν_E^R must be used to classify such systems further. It dictates how the edge states would be distributed over the left and right boundaries. We then naively extend the criteria to the cases that the quasi-Hermitian condition is violated. For all the cases that we consider no inconsistency has been found.

PACS numbers: 73.20.At,74.25.F-,73.63.Fg

I. Introduction

Topological materials have been at the center of attention in the community of condensed matter physicists since their discovery [1, 2]. Bulk–boundary correspondence (BBC) is arguably the most distinct among all the intriguing properties of topological insulators and superconductors. It is well known that they may be classified into a “periodic table” according to the symmetries and dimensionalities of the system [3–5]. Topological invariants associated with the Bloch bands of a system may be used to tell whether the system is in the topological phase. Moreover, it dictates the number of edge states that appear on the system’s boundaries.

The Su–Schrieffer–Heeger (SSH) model is the simplest topological insulator [6]. Originally, it was proposed to model a dimerized polyacetylene chain. It has also been realized using various systems. See Ref. [7] and references therein for details. The one-dimension (1D) winding number ν is the topological invariant that may be used to predict the number of edge states on the boundaries of the system. It is known that the 1D winding number is closely related to the Zak phase, γ [8], which is basically similar to the Berry phase [9]. It has been measured directly using a dimerized optical lattice [10].

Because of its simplicity, the SSH model has been one of the favorite prototypes to study topological insulators. First by adding an on-site energy term in the SSH model, one may extend it to the Rice–Mele model [11]. One may then use it to relate the SSH model to a Chern insulator by considering a charge-pumping process in such a system [12–14]. One may also add more “atoms” in a unit cell. As a result, there could be more than one occupied band in the system [15–17] and holonomies or equivalently, Wilson-loop, may be used to describe the topology of such a system [18, 19]. This is effectively the non-Abelian generalization of the Berry phase [8, 9]. Another interesting generalization is to introduce third-nearest-neighbor hopping amplitudes in the system. Such systems would admit topological phases with higher winding numbers, and they are referred to as the extended SSH models. It is known that there is an ambiguity in defining the Zak phase due to its dependence on the real-space origin and unit cell [20, 21]. Although a proposal that resolves such an ambiguity in the SSH model has been put forward, this kind of difficulty remains for extended SSH models, since the *intercellular* Zak phase from a band may be as large as 2π [20, 21]. Consequently, extended SSH models could serve as an arena to study such ambiguity.

Although the Hamiltonian of a closed system is typically Hermitian so that unitarity is preserved, real physical systems are usually coupled to their environment. Therefore, dissipative processes generally exist and the effective Hamiltonian would become non-Hermitian (NH). In fact, an effective NH Hamiltonian approach provides a simple and intuitive way to describe open systems and thus has been broadly used in electrical circuits, optical and mechanical systems, etc. See Ref. [22, 23] and references therein. In the past few years, there has been a growing interest in NH topological systems motivated by experimental observation of topological states in dissipative systems [26–35].

^a e-mail address: jackyphys@gmail.com

^b e-mail address: s963037@gmail.com

^c e-mail address: jihshihyou@ntnu.edu.tw

^d e-mail address: haochun71@yahoo.com.tw

^e e-mail address: hckao@phy.ntnu.edu.tw

Many surprises appear when one extends a Hermitian topological system to its NH counterpart [22–25]. First of all, the energy spectrum for a system with periodic boundary conditions (PBCs) is generally very different from that with open boundary conditions (OBCs) [36]. Since the energy spectrum of an NH system is generally complex, a new topological invariant, the spectral winding number, has been introduced [37, 38]. It has been incorporated to derive an NH counterpart of the periodic table of topological insulators [39]. Secondly, there is also the skin effect and hence even the wave functions of “bulk” states have an exponential damping or growing factor [40–43]. This in turn will lead to the breakdown of the conventional BBC [22, 40, 42, 44]. In an effort to generalize the BBC, the generalized Brillouin zone (BZ) has been introduced [43, 45–48]. It has been shown that using the generalized BZ, one can obtain the correct winding number for NH topological systems and reestablish the BBC. In Ref. [40], the authors propose the idea of biorthogonal BBC, which is then further generalized [49, 50]. They study the NH SSH model and its extension to demonstrate that the biorthogonal polarization may be used to determine the total number of edge states on the boundaries of the topological systems [40]. Although generalized BZ and biorthogonal polarization are useful to restore the BBC in NH systems [51], it is still worthwhile to seek a classification based only on the suitably modified winding number, $\bar{\nu}$, and spectral winding numbers, ν_E^L and ν_E^R , along the same lines as in Ref. [37, 38]. For this purpose, we study in detail the quasi-Hermitian (QH) limit of the NH extended SSH models with next-to-nearest neighbor hopping amplitudes. In such a limit, the system may be mapped to a Hermitian one. As a result, the energy spectrum is real and we can use a simple modified winding number to classify the topological phases of the system.

The rest of the paper is organized in the following way. In Sec. II, we first use the NH SSH model to carry out a detailed analysis of its secular and characteristic equations. Based on the study, we conclude the NH SSH model may be mapped to a Hermitian one. In other words, it is pseudo-Hermitian (PH) [52]. Moreover, one can use the modified winding number, $\bar{\nu}$, and spectral winding number ν_E to reestablish the BBC. In particular, $\bar{\nu}$ may be used to determine the total number of edge states on the boundaries, while ν_E dictates how the edge states would distribute over the left and right boundaries. The results obtained are confirmed using numerical calculation and are consistent with those found in the literature [40–43, 49, 50, 53]. Next, we try to establish the so-called quasi-Hermitian condition (QHC), under which this may be generalized to the NH extended SSH models. When QHC is satisfied, we again show explicitly in terms of the system’s secular and characteristic equations that it may be mapped to a Hermitian one. After some analysis, we show that one may still use $\bar{\nu}$, ν_E^L and ν_E^R to reestablish the BBC. The results are also verified using numerical calculation. In Sec. IV, we carry out a study of general NH extended SSH models. Again we analytically find the characteristic equation and numerically calculate the energy spectrum of such systems. Here, we naively extend the criteria that we obtained in the quasi-Hermitian (QH) limit and check whether they still hold. Finally, we make conclusions and discuss possible extensions in Sec. V.

II. NH SSH model

Let’s begin with a finite chain of NH SSH models with OBCs:

$$H_{\text{SSH}} = \sum_{j=1}^{N-1} \left\{ (t_0^L A_j^\dagger + t_1^R A_{j+1}^\dagger) B_j + (t_0^R A_j + t_1^L A_{j+1}) B_j^\dagger \right\} + t_0^L A_N^\dagger B_N + t_0^R A_N B_N^\dagger. \quad (1)$$

There are N unit cells in the system, and j is used to denote them. $t_0^{L,R}, t_1^{L,R}$ are the intra-cell and inter-cell left and right hopping amplitudes, respectively. It is straightforward to obtain the equation of motion (EOM) satisfied by the energy eigenstates:

$$\begin{aligned} EA_j - (t_0^L B_j + t_1^R B_{j-1}) &= 0, & \text{for } j = 2, \dots, N; \\ EB_j - (t_0^R A_j + t_1^L A_{j+1}) &= 0, & \text{for } j = 1, \dots, N-1. \end{aligned} \quad (2)$$

The boundary conditions (BCs) are specified by

$$\begin{aligned} EA_1 - t_0^L B_1 &= 0; \\ EB_N - t_0^R A_N &= 0, \end{aligned} \quad (3)$$

which may be simplified to

$$\begin{aligned} B_0 &= 0; \\ A_{N+1} &= 0. \end{aligned} \quad (4)$$

To find the solutions to the system, we let

$$A_j = \alpha s^j, B_j = \beta s^j, \quad (5)$$

and it would lead to

$$\begin{aligned} E\alpha - (t_0^L + t_1^R s^{-1})\beta &= 0, \\ E\beta - (t_0^R + t_1^L s)\alpha &= 0. \end{aligned} \quad (6)$$

Non-trivial solutions for α and β exist only if the determinant formed by the coefficients of α and β is vanishing, i.e.

$$E^2 - (t_0^L + t_1^R s^{-1})(t_0^R + t_1^L s) = 0, \quad (7)$$

which we call the secular equation. Since the above equation is quadratic in s , the most general solutions of A_j and B_j to eq. (6) are given by

$$A_j = \alpha_1 s_1^j + \alpha_2 s_2^j, B_j = \beta_1 s_1^j + \beta_2 s_2^j. \quad (8)$$

Here, s_1 and s_2 are the two roots of the secular equation in eq. (7). Obviously, the product and sum of the two roots satisfy the following relations:

$$\begin{aligned} s_1 s_2 &= t_0^R t_1^R / (t_0^L t_1^L), \\ s_1 + s_2 &= (E^2 - t_0^L t_0^R - t_1^L t_1^R) / (t_0^L t_1^L). \end{aligned}$$

Substituting the above expressions back to the BCs given in eq. (4) and then expressing α_1, α_2 in terms of β_1, β_2 , we see the BCs may be simplified to

$$\begin{aligned} t_1^R \beta_1 + t_1^R \beta_2 &= 0; \\ t_1^L s_1^N (t_0^L s_1 + t_1^R) \beta_1 + t_1^L s_2^N (t_0^L s_2 + t_1^R) \beta_2 &= 0. \end{aligned} \quad (9)$$

Again, non-trivial solutions for β_1 and β_2 exist only if the determinant consisting of the coefficients of β_1 and β_2 in the above equations is vanishing:

$$t_1^R t_1^L (s_1^N - s_2^N) + t_0^R t_0^L (s_1^{N+1} - s_2^{N+1}) = 0, \quad (10)$$

which we call the characteristic equation of s hereafter. Define the skin effect factor

$$r = \sqrt{t_0^R t_1^R / (t_0^L t_1^L)}, \quad (11)$$

so that $s_1 = r\bar{s}, s_2 = r\bar{s}^{-1}$, and the above equation may be cast into the following form:

$$\bar{t}_0 U_N(\bar{u}) + \bar{t}_1 U_{N-1}(\bar{u}) = 0. \quad (12)$$

Here, $\bar{t}_0 = \sqrt{t_0^R t_0^L}$ and $\bar{t}_1 = \sqrt{t_1^R t_1^L}$. $\bar{u} = (\bar{s} + \bar{s}^{-1})/2$ and $U_N(\bar{u})$ is the Chebyshev polynomials of the second kind of degree N , which has also been mentioned in Ref. [54]. Note that the above equation is equivalent to that in the Hermitian case when we identify the variables properly. From Eq. (9), we see the energy of the system is always real, with its spectrum given by

$$E = \pm (\bar{t}_0^2 + \bar{t}_1^2 + 2\bar{t}_0 \bar{t}_1 \bar{u})^{1/2}. \quad (13)$$

From our experience with the Hermitian SSH model, it is straightforward to come to the conclusion that the system would be in the topological phase if $\bar{t}_1/\bar{t}_0 > 1$. In this case, there exist two solutions of \bar{s} , that give rise to two almost zero energy edge states. They are approximately \bar{s}_0 and \bar{s}_0^{-1} with $\bar{s}_0 = -\bar{t}_0/\bar{t}_1$. Since now it is the ratio \bar{t}_0/\bar{t}_1 that determines whether the system is in the topological phase, it is now the modified winding number, $\bar{\nu}$, that plays the role of topological invariant. We expect that $\bar{\nu}$ is determined by whether $h(p) = \bar{t}_0 + \bar{t}_1 e^{ip}$ wrap around the origin when p ranges over the BZ. Furthermore, it is known that there is the so-called ‘‘skin effect’’ in the NH SSH model, which may be described by the parameter r defined in eq. (11). The most striking feature here is that even the ‘‘bulk’’ states would exhibit exponential growing or damping behavior in general. For $r > 1$ and $r < 1$, all the ‘‘bulk’’ states would be ‘‘tilted’’ to the right and left boundaries, respectively. Because of this effect, the exponential factors of the

edge states become $r\bar{s}_0, \approx -(t_0^R/t_1^L)$ and $r\bar{s}_0^{-1} \approx -(t_1^R/t_0^L)$. In the topological phase, if both t_0^R/t_1^L and t_1^R/t_0^L are smaller (larger) than 1, then both two edge states would appear on the left (right) boundary, in stark contrast with the Hermitian case. We would also like to mention that even if $t_1^R/t_0^L < 1$ the edge state associated with $s = -t_1^R/t_0^L$ would not exist in a right semi-infinite chain, different from the one associated with $s = -t_0^R/t_1^L$.

These results may be confirmed numerically, and the spectrum and wave functions of the edge states are shown in Fig. 1. Here, we choose $N = 20$, $(t_0^L, t_0^R, t_1^L, t_1^R) = (1, 4, 3, 3)$ so that $(\bar{t}_0, \bar{t}_1) = (2, 3)$, $r = 2$ and $\bar{\nu} = 1$. At first glance, it seems that both edge states, ψ_1 and ψ_2 , are non-vanishing only on the B sites and they form a chiral conjugate pair. This is of course a reflection of the skin effect, but it is in fact misleading and arises from the limitation in numerical accuracy. This may be seen by taking the difference and sum of the wave functions of the two edge states, ψ_1 and ψ_2 . The resulting wave functions correspond to two right edge states. The former one is non-vanishing on B sites only and the latter one is on A sites only. This is a signature that they are derived from the Hermitian SSH model.

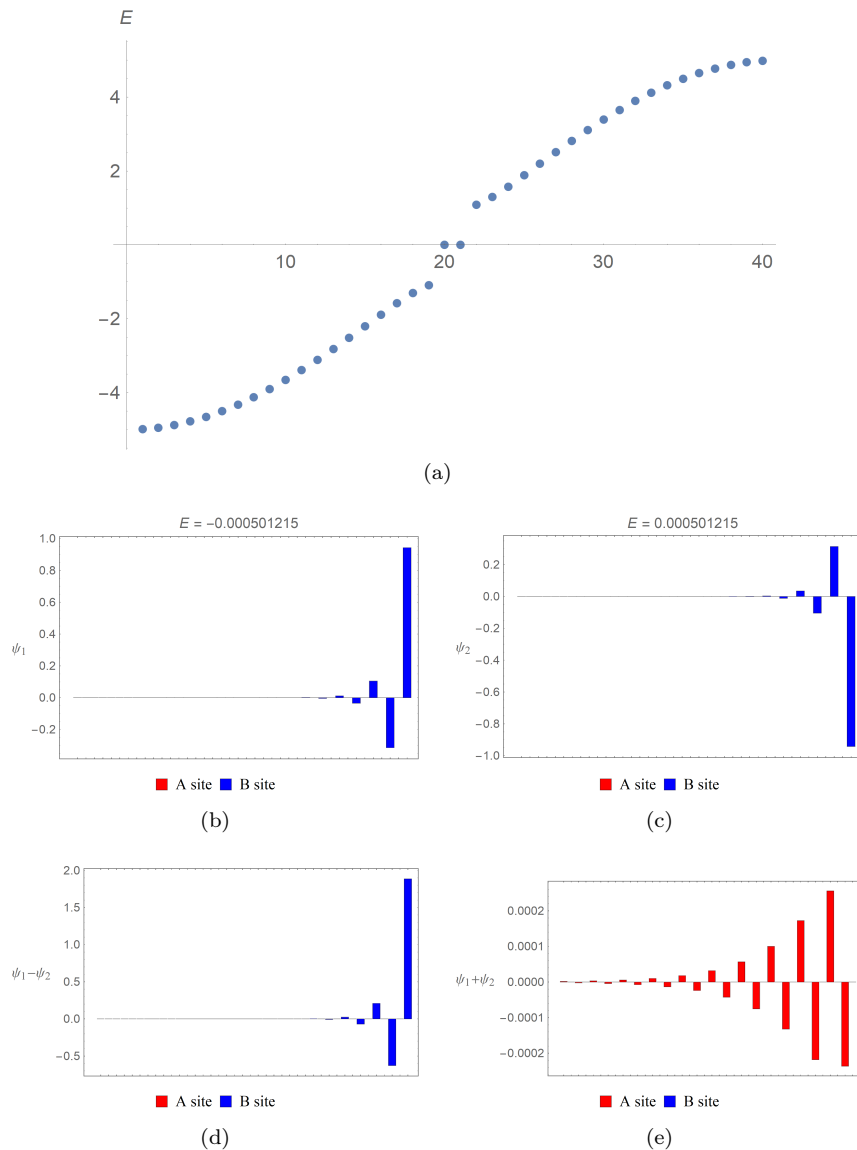


FIG. 1. (a) The energy spectrum in the topological phase of the NH SSH model, where $(t_0^L, t_0^R, t_1^L, t_1^R) = (1, 4, 3, 3)$. The energies of the two edge states ψ_1, ψ_2 are both approximately zero. (b), (c) The wave functions of the two edge states in the system. Note that they are both right edge states. (d), (e) The wave functions of the difference and sum of ψ_1 and ψ_2 . Note that although $\psi_1 + \psi_2$ is also a right edge state, it is non-vanishing only on the A sites in contrast to $\psi_1 - \psi_2$.

As shown above, although $\bar{\nu}$ may tell us the total number of edge states in the system, the edge states now may no longer distribute evenly on the left or right boundaries in contrast to the Hermitian case. To further classify the topological phase, we must consider the case with PBCs to see how to determine which boundaries the edge states

would show up. Under such BCs, we have

$$s_k = \exp(i2\pi k/N), \text{ and } E = \pm (t_0^L t_0^R + t_1^L t_1^R + t_0^L t_1^L s_k + t_0^R t_1^R s_k^{-1})^{1/2}, \quad (14)$$

with $k = 0, 1, \dots, N-1$. It is obvious that the energy is generally complex and the spectrum is very different from that of the OBC case. In the continuum limit, we have

$$\det H(p) = E^2(p) = (t_0^R + t_1^L e^{ip}) (t_0^L + t_1^R e^{-ip}), \quad (15)$$

where $p \in (-\pi, \pi]$. Since $\det H(p)$ is a product of two factors, the spectral winding number ν_E for its trajectory on the complex plane is given by

$$\nu_E = \nu_E^R + \nu_E^L. \quad (16)$$

Here ν_E^L is the spectral winding number corresponding to the factor $(t_0^R + t_1^L e^{ip})$, and ν_E^R corresponding to $(t_0^L + t_1^R e^{-ip})$. It is ν_E that will determine how the edge states would be distributed over the two boundaries.

1) $\bar{\nu} = 1$:

- i) $\nu_E = 1$ ($t_0^L > t_1^R, t_0^R < t_1^L$). Both edge states appear on the left boundary.
- ii) $\nu_E = 0$ ($t_0^L < t_1^R, t_0^R < t_1^L$). One edge state appears on the left boundary and the other on the right.
- iii) $\nu_E = -1$ ($t_0^L < t_1^R, t_0^R > t_1^L$). Both edge states appear on the right boundary.

2) $\bar{\nu} = 0$: $\nu_E = 1, 0, -1$. There is no edge state.

The modified winding number $\bar{\nu}$ may also be obtained using the so-called modified PBCs [55]. Of course, it is equivalent to using a generalized BZ so that $\bar{\nu} = \nu_E|_{C_s}$, where C_s is a circle about the origin with radius equal to the skin effect factor r [43, 47, 48]. As we shall see, this criterion may also be generalized to the NH extended SSH models.

III. Quasi-Hermitian Extended SSH models

Let's now turn to the NH extended SSH models, again with OBCs. To be specific, we first consider the type 1 case, and the Hamiltonian for a finite chain is given by

$$H_{\text{ext1}} = \sum_{j=1}^{N-2} \left\{ (t_0^L A_j^\dagger + t_1^R A_{j+1}^\dagger + t_2^R A_{j+2}^\dagger) B_j + (t_0^R A_j + t_1^L A_{j+1} + t_2^L A_{j+2}) B_j^\dagger \right\} \\ + (t_0^L A_{N-1}^\dagger + t_1^R A_N^\dagger) B_{N-1} + (t_0^R A_{N-1} + t_1^L A_N) B_{N-1}^\dagger + t_0^L A_N^\dagger B_N + t_0^R A_N B_N^\dagger. \quad (17)$$

Again, j denotes the unit cell and there are N unit cells in total. In addition to $t_0^{L,R}$ and $t_1^{L,R}$, now we also have $t_2^{L,R}$, the third-nearest-neighbor left and right hopping amplitudes. It is straightforward to obtain the EOM:

$$EA_j - (t_0^L B_j + t_1^R B_{j-1} + t_2^R B_{j-2}) = 0, \quad \text{for } j = 3, \dots, N; \\ EB_j - (t_0^R A_j + t_1^L A_{j+1} + t_2^L A_{j+2}) = 0, \quad \text{for } j = 1, \dots, N-2, \quad (18)$$

and BCs after some algebra

$$B_{-1} = B_0 = 0; \\ A_{N+1} = A_{N+2} = 0. \quad (19)$$

By substituting $A_j = \alpha s^j, B_j = \beta s^j$ into the EOM, we obtain

$$E\alpha - (t_0^L + t_1^R s^{-1} + t_2^R s^{-2})\beta = 0, \\ E\beta - (t_0^R + t_1^L s + t_2^L s^2)\alpha = 0, \quad (20)$$

and hence the secular equation:

$$E^2 - (t_0^L + t_1^R s^{-1} + t_2^R s^{-2})(t_0^R + t_1^L s + t_2^L s^2) = 0. \quad (21)$$

Since the above equation is quartic in s , the most general solutions of A_j and B_j would be given by

$$A_j = \sum_{I=1}^4 \alpha_I s_I^j, B_j = \sum_{I=1}^4 \beta_I s_I^j. \quad (22)$$

Here, s_1, s_2, s_3 and s_4 are the four roots of the secular equation, and they satisfy the following relations:

$$\begin{aligned} s_1 s_2 s_3 s_4 &= t_0^R t_2^R / (t_0^L t_2^L), \\ s_1 s_2 s_3 + s_1 s_2 s_4 + s_1 s_3 s_4 + s_2 s_3 s_4 &= - (t_0^R t_1^R + t_1^L t_2^R) / (t_0^L t_2^L), \\ s_1 s_2 + s_1 s_3 + s_1 s_4 + s_2 s_3 + s_2 s_4 + s_3 s_4 &= (t_0^L t_0^R + t_1^L t_1^R + t_2^L t_2^R - E^2) / (t_0^L t_2^L), \\ s_1 + s_2 + s_3 + s_4 &= - (t_0^L t_1^L + t_1^R t_2^L) / (t_0^L t_2^L). \end{aligned} \quad (23)$$

By using the most general forms of A_j and B_j , the BCs given in eqs. (19) becomes

$$\begin{aligned} \beta_1 s_1^{-1} + \beta_2 s_2^{-1} + \beta_3 s_3^{-1} + \beta_4 s_4^{-1} &= 0, \\ \beta_1 + \beta_2 + \beta_3 + \beta_4 &= 0, \\ \alpha_1 s_1^{N+1} + \alpha_2 s_2^{N+1} + \alpha_3 s_3^{N+1} + \alpha_4 s_4^{N+1} &= 0, \\ \alpha_1 s_1^{N+2} + \alpha_2 s_2^{N+2} + \alpha_3 s_3^{N+2} + \alpha_4 s_4^{N+2} &= 0. \end{aligned} \quad (24)$$

The criteria obtained in the previous section are all very nice but one would see in no time that it is impossible to generalize them directly to the extended SSH models. Therefore, we will limit ourselves to the special case that there is only one single skin effect factor

$$r = [t_0^R t_2^R / (t_0^L t_2^L)]^{1/4}, \quad (25)$$

such that $s_1 = r \bar{s}_1, s_2 = r \bar{s}_2, s_3 = r \bar{s}_1^{-1}$, and $s_4 = r \bar{s}_2^{-1}$. This may be achieved when the following condition is satisfied

$$(t_0^R t_1^R + t_1^L t_2^R) = r^2 (t_0^L t_1^L + t_1^R t_2^L),$$

which may be simplified to

$$t_1^L = t_1^R \sqrt{t_0^R t_2^L / (t_0^L t_2^R)}. \quad (26)$$

Because of this additional constraint, only five of the six parameters are independent. When this occurs, we expect that the system may be mapped to a Hermitian type 1 extended SSH model, and all the energy eigenvalues would be real. For this reason, we will call this constraint the quasi-Hermiticity condition (QHC). Note that quasi-Hermiticity is only a subset of pseudo-Hermiticity since there obviously exist NH extended systems that do not satisfy the QHC but still have a real energy spectrum.

Now, let's show explicitly how the system may be mapped to a Hermitian type 1 extended SSH model when the QHC is satisfied. First, we would like to mention that when this is the case, only two of the equations in eqs. (23) are independent. They may be reduced to the following forms:

$$\begin{aligned} \bar{u}_1 + \bar{u}_2 &= - (t_0^L t_1^L + t_1^R t_2^L) / (2r t_0^L t_2^L), \\ 2 + 4\bar{u}_1 \bar{u}_2 &= (t_0^L t_0^R + t_1^L t_1^R + t_2^L t_2^R - E^2) / (r^2 t_0^L t_2^L), \end{aligned} \quad (27)$$

in terms of $\bar{u}_1 = (\bar{s}_1 + \bar{s}_1^{-1})/2$ and $\bar{u}_2 = (\bar{s}_2 + \bar{s}_2^{-1})/2$. Upon using eqs. (20), we see $\alpha_I = \{(t_0^L + t_1^R s_I^{-1} + t_2^R s_I^{-2})/E\} \beta_I$, with $I = 1, \dots, 4$. After some algebra, the characteristic equation for \bar{s} may be obtained from the condition that the determinant formed by the coefficients of β_1, \dots, β_4 in eqs. (24) is vanishing:

$$\begin{aligned} &\{\bar{t}_0 U_{N+2}(\bar{u}_1) + \bar{t}_1 U_{N+1}(\bar{u}_1) + \bar{t}_2 U_N(\bar{u}_1)\} \{\bar{t}_0 U_N(\bar{u}_2) + \bar{t}_1 U_{N-1}(\bar{u}_2) + \bar{t}_2 U_{N-2}(\bar{u}_2)\} \\ &+ \{\bar{t}_0 U_{N+2}(\bar{u}_2) + \bar{t}_1 U_{N+1}(\bar{u}_2) + \bar{t}_2 U_N(\bar{u}_2)\} \{\bar{t}_0 U_N(\bar{u}_1) + \bar{t}_1 U_{N-1}(\bar{u}_1) + \bar{t}_2 U_{N-2}(\bar{u}_1)\} \\ &- 2 \{\bar{t}_0 U_{N+1}(\bar{u}_1) + \bar{t}_1 U_N(\bar{u}_1) + \bar{t}_2 U_{N-1}(\bar{u}_1)\} \{\bar{t}_0 U_{N+1}(\bar{u}_2) + \bar{t}_1 U_N(\bar{u}_2) + \bar{t}_2 U_{N-1}(\bar{u}_2)\} \\ &+ 2 \{\bar{t}_0^2 + \bar{t}_1^2 + \bar{t}_2^2 - 2\bar{t}_0 \bar{t}_2 (1 + 2\bar{u}_1 \bar{u}_2)\} = 0. \end{aligned} \quad (28)$$

Similar to the case of the NH SSH model, we have further introduced $\bar{t}_2 = \sqrt{t_2^L t_2^R}$. In terms of \bar{t}_0, \bar{t}_1 and \bar{t}_2 , eq. (27) becomes

$$\bar{u}_1 + \bar{u}_2 = -\bar{t}_1 (\bar{t}_0 + \bar{t}_2) / (2\bar{t}_0 \bar{t}_2),$$

$$E^2 = \bar{t}_0^2 + \bar{t}_1^2 + \bar{t}_2^2 + 2\bar{t}_0\bar{t}_2(2 + 4\bar{u}_1\bar{u}_2). \quad (29)$$

The above characteristic equation is exactly the same as the one obtained in Ref. [56] if we identify the parameters $(\bar{t}_0, \bar{t}_1, \bar{t}_2)$ with (t_0, t_1, t_2) .

By substituting the first part in the above equation into eq. (28), we obtain a characteristic equation in terms of \bar{u}_1 which is a polynomial of degree $2N + 2$. By closer examination, we see that there is an additional factor $[\bar{u}_1 + \bar{t}_1(\bar{t}_0 + \bar{t}_2)/(4\bar{t}_0\bar{t}_2)]^2$ in the characteristic equation, which does not correspond to any physical states and can be ignored. Since both equations are symmetric with respect to \bar{u}_1 and \bar{u}_2 , we may always require $\bar{u}_1 > \bar{u}_2$ to remove the redundancy in the solutions of \bar{u}_1 and \bar{u}_2 . Note that here \bar{u}_1 and \bar{u}_2 are generally complex, and the relation $\bar{u}_1 > \bar{u}_2$ is defined by $\text{Re}\{\bar{u}_1\} > \text{Re}\{\bar{u}_2\}$ or $\text{Re}\{\bar{u}_1\} = \text{Re}\{\bar{u}_2\}$ and $\text{Im}\{\bar{u}_1\} > \text{Im}\{\bar{u}_2\}$. Eventually, we find N roots of u_1 consistent with what we expected. We would like to mention that by solving the characteristic equation in eq. (28), we may also obtain the energy spectrum, which agrees completely with that achieved by numerical diagonalization.

Analogous to the Hermitian case, the edge states have almost zero energy, and the characteristic s 's associated with these states satisfy the condition in eq. (20) and $\beta \approx 0$. This gives rise to

$$t_0^R + t_1^L s + t_2^L s^2 \approx 0, \quad (30)$$

$$t_0^L + t_1^R s^{-1} + t_2^R s^{-2} \approx 0. \quad (31)$$

In terms of \bar{s} , the first one leads to the following quadratic relation

$$\bar{t}_0 + \bar{t}_1\bar{s} + \bar{t}_2\bar{s}^2 \approx 0. \quad (32)$$

Thus, the system may be classified according to the modified winding number $\bar{\nu}$, which dictates in the above quadratic equation the number of roots with absolute values less than 1, just like in the Hermitian case [56]. It is known that there are three different phases, and we expect that $\bar{\nu}$ would also determine the total number of edge states on the system's boundaries.

- 1) $\bar{t}_2 + \bar{t}_0 > \bar{t}_1$, and $\bar{t}_2 > \bar{t}_0$: The system is in the topological phase with $\bar{\nu} = 2$. There are four edge states in total on the boundaries.
- 2) $\bar{t}_2 + \bar{t}_0 < \bar{t}_1$: The system is in the topological phase with $\bar{\nu} = 1$. There are two edge states in total on the boundaries.
- 3) $\bar{t}_2 + \bar{t}_0 > \bar{t}_1$, and $\bar{t}_2 < \bar{t}_0$: The system is in the trivial phase with $\bar{\nu} = 0$. There are no edge states.

Again, this may also be obtained using a generalized BZ or modified PBCs [43, 47, 48, 55].

Because of the skin effect, the edge states may not be evenly distributed over the left and right boundaries. Similar to the NH SSH model, we may use ν_E to determine where they would reside. In the continuum limit, we have from eq. (21)

$$E^2(p) = (t_0^R + t_1^L e^{ip} + t_2^L e^{2ip})(t_0^L + t_1^R e^{-ip} + t_2^R e^{-2ip}). \quad (33)$$

Again, we have $\nu_E = \nu_E^L + \nu_E^R$, with ν_E^L the spectral winding number corresponding to the factor $(t_0^R + t_1^L e^{ip} + t_2^L e^{2ip})$, and ν_E^R corresponding to $(t_0^L + t_1^R e^{-ip} + t_2^R e^{-2ip})$. Just like in the Hermitian case, the number of solutions to eqs. (30) and (31) that have magnitudes smaller or larger than 1 indicates the possible numbers of edge states on the left and right boundaries, respectively. In addition, we must bear in mind that the total number of edge states is $2\bar{\nu}$. Now, let's summarize the correspondence between (ν_E^L, ν_E^R) and the locations of the edge states:

- 1) $\bar{\nu} = 2$:
 - i) $\nu_E = 2$. All four edge states are on the left boundary.
 - ii) $\nu_E = 1$. Three edge states are on the left boundary and one on the right.
 - iii) $\nu_E = 0$. Two edge states are on the left boundary and two on the right.
 - iv) $\nu_E = -1$. One edge state is on the left boundary and three on the right.
 - v) $\nu_E = -2$. All four edge states are on the right boundary.
- 2) $\bar{\nu} = 1$:
 - i) $(\nu_E^L, \nu_E^R) = (2, 0), (1, 0), \boxed{(2, -1)}$. Both edge states are on the left boundary.

ii) $(\nu_E^L, \nu_E^R) = \boxed{(2, -1)}, (2, -2), (1, -1), (0, 0), \boxed{(1, -2)}$. One edge state is on the left boundary and one is on the right.

iii) $(\nu_E^L, \nu_E^R) = \boxed{(1, -2)}, (0, -1), (0, -2)$. Both edge states are on the right boundary.

3) $\bar{\nu} = 0$: $\nu_E = 2, 1, 0, -1, 2$. No edge state.

Note that we put a box around $(2, -1)$ and $(1, -2)$ to indicate that there is an ambiguity in determining the locations of the edge states when (ν_E^L, ν_E^R) equal to these values.

From eqs. (25) and (26), we see if $(t_0^L, t_0^R, t_1^L, t_1^R, t_2^L, t_2^R)$ satisfy the QHC and they are scaled in the following way:

$$\begin{aligned} (t_0^L, t_1^R, t_2^R) &\rightarrow (\tilde{r}^{-1}t_0^L, t_1^R, \tilde{r}t_2^R), \\ (t_0^R, t_1^L, t_2^L) &\rightarrow (\tilde{r}t_0^R, t_1^L, \tilde{r}^{-1}t_2^L), \end{aligned} \quad (34)$$

then $(\bar{t}_0, \bar{t}_1, \bar{t}_2)$ would remain the same, while the skin effect factor will change by a factor of \tilde{r} . Since the characteristic equation and energy spectrum only depend on $(\bar{t}_0, \bar{t}_1, \bar{t}_2)$, they are also invariant under the scaling. Thus, it is a symmetry of the NH extended SSH models. In particular, we may use \tilde{r} to scale the magnitude of the $(s_I)'s$ corresponding to the edge states. Hence we may vary the value of ν_E between -2 and 2 . In fact, this scaling symmetry remains intact even in general NH extended SSH models. If we can use the scaling to make ν_E zero, the edge states the trajectory of E will enclose all the ‘‘bulk’’ states so it gives us another way to identify the edge states in the system, especially when we consider general NH extended SSH models.

With caution, all the previous predictions may be confirmed numerically. First, we consider the case that there are 40 sites with the parameters chosen to be $(t_0^L, t_0^R, t_1^L, t_1^R, t_2^L, t_2^R) = (1/2, 1/8, 2, 2, 4, 1)$. Hence, $(\bar{t}_0, \bar{t}_1, \bar{t}_2) = (1/4, 2, 2)$, $\bar{\nu} = 2$, $r = 1/2$ and $(\nu_E^L, \nu_E^R) = (2, -1)$. There are four edge states, which we call $\psi_1, \psi_2, \psi_3, \psi_4$ in the order of increasing energy, with (ψ_1, ψ_4) and (ψ_2, ψ_3) forming two chiral conjugate pairs. They all have almost zero energies and there are indeed three on the left boundary and one on the right. However, due to the limitation of numerical accuracy, it is difficult to see this directly from their wave functions. To see this explicitly, we must consider the following linear combination: $\psi_1 - \psi_4, \psi_1 + \psi_4, \psi_2 - \psi_3, \psi_2 + \psi_3$. From these linear combinations of wave functions, we also see that two of them are non-vanishing on the A sites only and two on the B sites only. Similar to the SSH case, this is evidence that they are derived from the Hermitian extended SSH model. The energy spectrum and wave functions of the edge states are shown in Fig. 2.

Next, we choose the parameters to be $(t_0^L, t_0^R, t_1^L, t_1^R, t_2^L, t_2^R) = (1/2, 8, 5, 5, 1/4, 4)$ so that $(\bar{t}_0, \bar{t}_1, \bar{t}_2) = (2, 5, 1)$, $\bar{\nu} = 1$, $r = 4$, and $(\nu_E^L, \nu_E^R) = (0, -1)$. There are two edge states, denoted by ψ_1 and ψ_2 , in the order of increasing energy. Again, they form a chiral conjugate pair. Due to the skin effect, they are both right edge states and seem to be non-vanishing only on the B sites. By taking the difference and sum of ψ_1 and ψ_2 , we indeed see that both edge states are on the right boundary. Again, one of the resultant wave functions is non-vanishing only on the A sites and the other non-vanishing on the B sites only. The energy spectrum and wave functions of the edge states are shown in Fig. 3,

A similar analysis may also be carried out for the NH type 2 extended SSH model satisfying the QHC. This kind of NH extended SSH model has been used extensively to investigate the general BZ in the literature [43, 47, 48]. We relegate the details to Appendix A to avoid repetition in the main text.

We may also consider the case that there are an odd number of sites in the NH extended SSH models so that there is one incomplete unit cell by the right boundary. Since this would change the BC on the right boundary, it would also change the number of edge states. Similarly, the details of the analysis are deferred to Appendix B.

IV. General NH extended SSH models

Let’s now consider a general NH type 1 extended SSH model. By introducing the variables $s_{12} = \sqrt{s_1 s_2}$, $u_{12} = (s_1 + s_2)/(2s_{12})$, and $s_{34} = \sqrt{s_3 s_4}$, $u_{34} = (s_3 + s_4)/(2s_{34})$, the characteristic equation may be written in terms

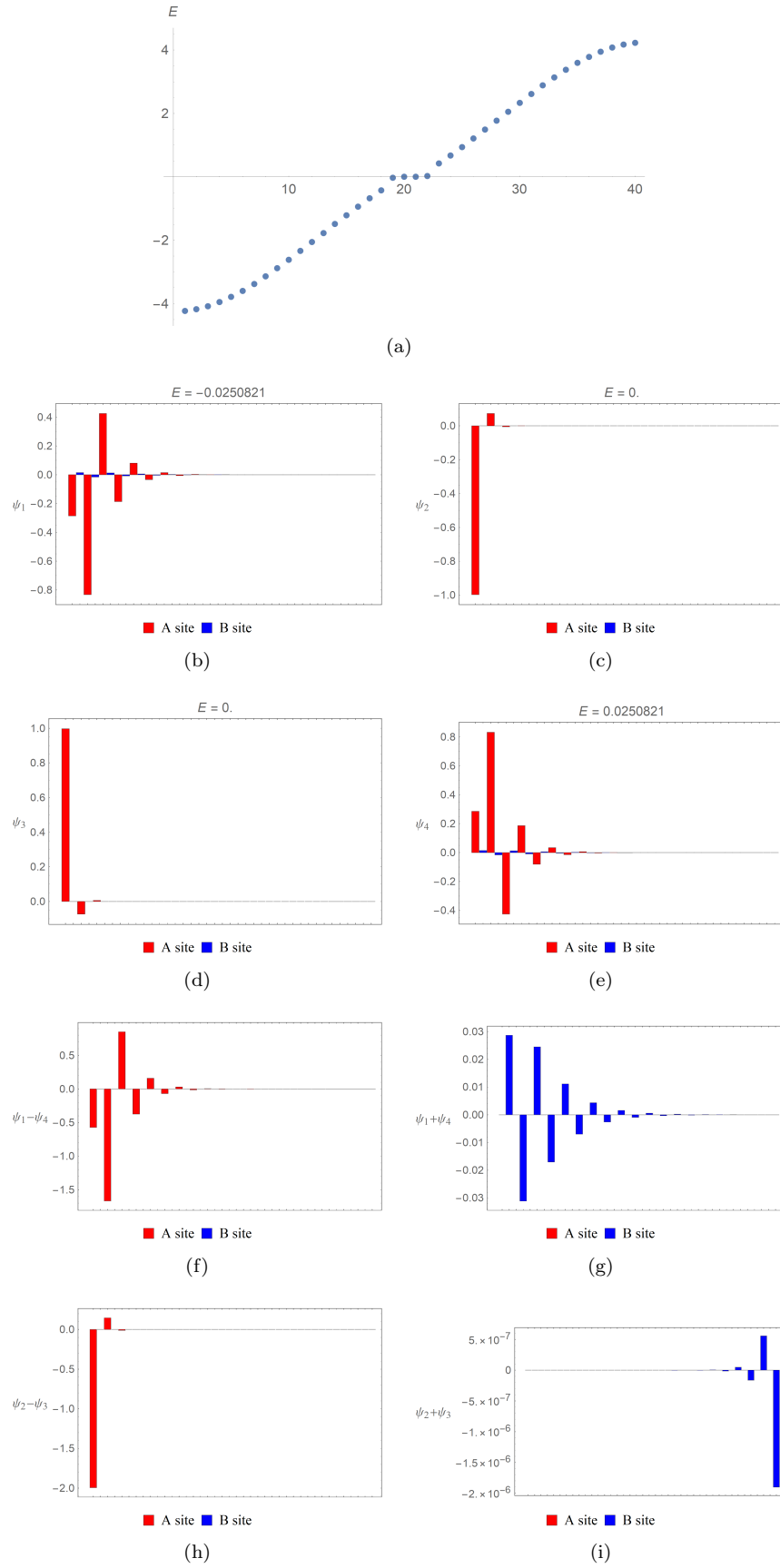


FIG. 2. (a) The energy spectrum of the NH type 1 extended SSH model with 40 sites, where $(t_0^L, t_0^R, t_1^L, t_1^R, t_2^L, t_2^R) = (1/2, 1/8, 2, 2, 4, 1)$. Thus, $(\bar{t}_0, \bar{t}_1, \bar{t}_2) = (1/4, 2, 2)$ and it is in the topological phase with $\bar{\nu} = 2$. (b), (c), (d), (e) The wave functions of the edge states $\psi_1, \psi_2, \psi_3, \psi_4$, which all have approximately zero energies. (f), (g) The difference and sum and of (ψ_1, ψ_4) . (h), (i) The difference and sum of (ψ_2, ψ_3) . Note that there are three and one edge states on the left and right boundaries, respectively. This is consistent with the fact that $\nu_E = 1$.

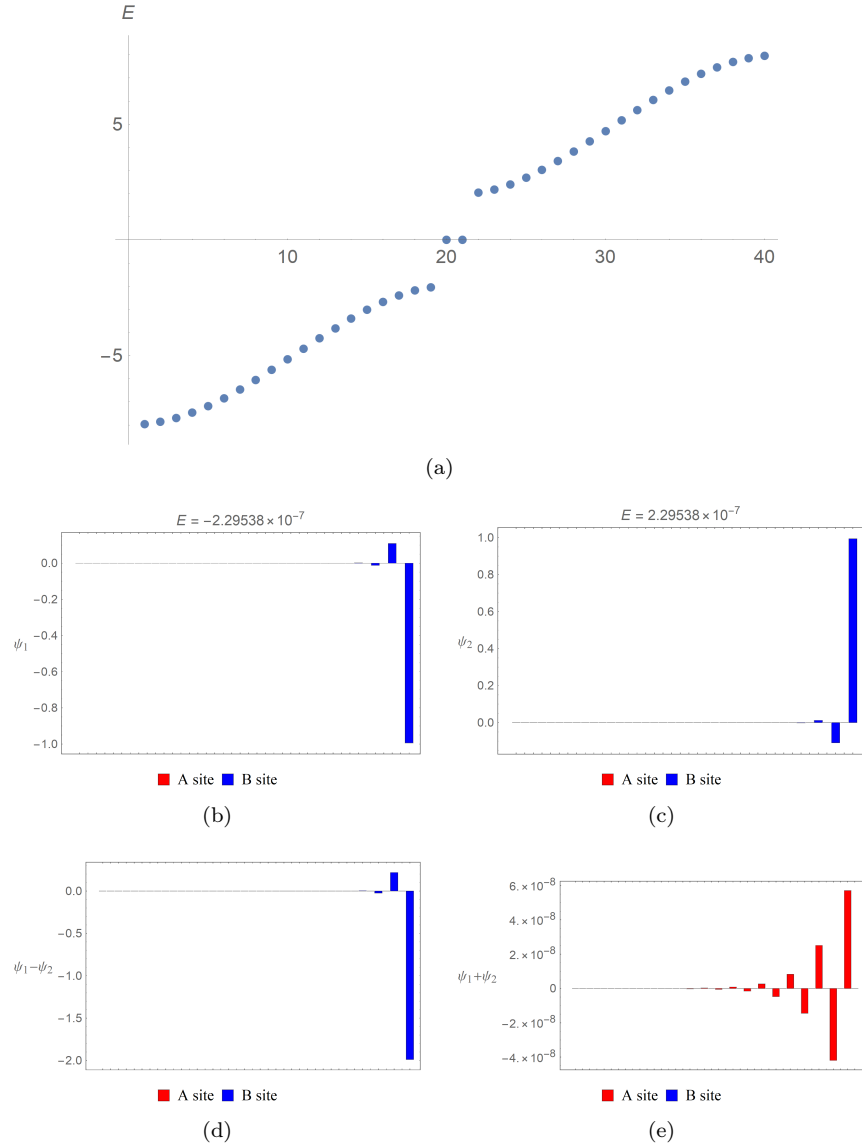


FIG. 3. (a) The energy spectrum of the NH type 1 extended SSH model with 40 sites, where $(t_0^L, t_0^R, t_1^L, t_1^R, t_2^L, t_2^R) = (1/2, 8, 5, 5, 1/4, 4)$. Thus, $(\bar{t}_0, \bar{t}_1, \bar{t}_2) = (2, 5, 1)$ and it is in the topological phase with $\bar{\nu} = 1$. The energies of the two edge states ψ_1, ψ_2 are both approximately zero. (b), (c) The wave functions of the two edge states in the system. (d), (e) The difference and sum of ψ_1 and ψ_2 . Note that both edge states are on the right boundary, consistent with the fact that $(\nu_E^L, \nu_E^R) = (0, -1)$.

of these variables:

$$\begin{aligned}
& \left\{ -t_0^L s_{12}^{N-3} s_{34}^{N+1} U_{N+1}(u_{34}) [t_0^L s_{12}^2 U_{N+1}(u_{12}) + t_1^R s_{12} U_N(u_{12}) + t_2^R U_{N-1}(u_{12})] \right. \\
& + t_0^L s_{12}^{N-2} s_{34}^N U_{N+2}(u_{34}) [t_0^L s_{12}^2 U_N(u_{12}) + t_1^R s_{12} U_{N-1}(u_{12}) + t_2^R U_{N-2}(u_{12})] \\
& + s_{12}^{N-3} s_{34}^N U_N(u_{34}) [(t_0^L)^2 s_{12}^3 U_{N+2}(u_{12}) + (t_0^L t_2^R - (t_1^R)^2) s_{12} U_N(u_{12}) - t_1^R t_2^R U_{N-1}(u_{12})] \\
& - s_{12}^{N-2} s_{34}^{N-1} U_{N+1}(u_{34}) [(t_0^L)^2 s_{12}^3 U_{N+1}(u_{12}) + (t_0^L t_2^R - (t_1^R)^2) s_{12} U_{N-1}(u_{12}) - t_1^R t_2^R U_{N-2}(u_{12})] \\
& + s_{12}^{N-3} s_{34}^{N-1} U_{N-1}(u_{34}) [t_0^L t_1^R s_{12}^3 U_{N+2}(u_{12}) - (t_0^L t_2^R - (t_1^R)^2) s_{12}^2 U_{N+1}(u_{12}) - (t_2^R)^2 U_{N-1}(u_{12})] \\
& - s_{12}^{N-2} s_{34}^{N-2} U_N(u_{34}) [t_0^L t_1^R s_{12}^3 U_{N+1}(u_{12}) - (t_0^L t_2^R - (t_1^R)^2) s_{12}^2 U_N(u_{12}) - (t_2^R)^2 U_{N-2}(u_{12})] \\
& + t_2^R s_{12}^{N-2} s_{34}^{N-2} U_{N-2}(u_{34}) [t_0^L s_{12}^2 U_{N+2}(u_{12}) + t_1^R s_{12} U_{N+1}(u_{12}) + t_2^R U_N(u_{12})] \\
& \left. - t_2^R s_{12}^{N-1} s_{34}^{N-3} U_{N-1}(u_{34}) [t_0^L s_{12}^2 U_{N+1}(u_{12}) + t_1^R s_{12} U_N(u_{12}) + t_2^R U_{N-1}(u_{12})] \right\} \\
& + s_{12}^{-2} s_{34}^{2N-2} \left\{ (t_2^R)^2 + 2t_1^R t_2^R s_{34} u_{34} + s_{34}^2 [(t_1^R)^2 + 2t_0^L t_2^R (2u_{34}^2 - 1)] + 2t_0^L t_1^R s_{34}^3 u_{34} + (t_0^L)^2 s_{34}^4 \right\} \\
& + s_{12}^{2N-2} s_{34}^{-2} \left\{ (t_2^R)^2 + 2t_1^R t_2^R s_{12} u_{12} + s_{12}^2 [(t_1^R)^2 + 2t_0^L t_2^R (2u_{12}^2 - 1)] + 2t_0^L t_1^R s_{12}^3 u_{12} + (t_0^L)^2 s_{12}^4 \right\} = 0. \tag{35}
\end{aligned}$$

From the second and fourth relations in eq. (23), we may express u_{12}, u_{34} in terms of s_{12}, s_{34} :

$$\begin{aligned}
u_{12} &= \frac{s_{12} s_{34} \{ t_0^L t_2^L (t_0^R t_1^R + t_1^L t_2^R) s_{34} - t_0^R t_2^R (t_0^L t_1^L + t_1^R t_2^L) s_{34}^{-1} \}}{2t_0^L t_0^R t_2^L t_2^R (s_{12}^2 - s_{34}^2)}, \\
u_{34} &= \frac{-s_{12} s_{34} \{ t_0^L t_2^L (t_0^R t_1^R + t_1^L t_2^R) s_{12} - t_0^R t_2^R (t_0^L t_1^L + t_1^R t_2^L) s_{12}^{-1} \}}{2t_0^L t_0^R t_2^L t_2^R (s_{12}^2 - s_{34}^2)}. \tag{36}
\end{aligned}$$

By making use of eq. (36), the characteristic equation may be written in terms of s_{12} and s_{34} . Furthermore, in terms of the skin effect factor r defined in eq. (25), we introduce $\bar{s}_{12} = s_{12}/r$ and $\bar{s}_{34} = s_{34}/r = \bar{s}_{12}^{-1}$. Finally, the characteristic equation may be written in terms of one single variable $\bar{u} = (\bar{s}_{12} + \bar{s}_{12}^{-1})/2$. It may be seen that the resulting expression is a polynomial in \bar{u} of degree $3N + 4$. When $N = 0$, we obtain a polynomial in \bar{u} of degree 4, whose solutions do not correspond to any physical states. It is, in fact, a common factor of the characteristic equation for arbitrary N , and thus can always be factored out and ignored. The fact that the final result for the characteristic equation is a polynomial in \bar{u} of degree $3N$ is derived from the permutation symmetry of s_1, \dots, s_4 . Again, the redundancy may be removed by requiring $s_1 \geq s_2 \geq s_3 \geq s_4$.

Let's first choose the parameters to be $(t_0^L, t_0^R, t_1^L, t_1^R, t_2^L, t_2^R) = (9/2, 2, 2, 2, 1, 9/4)$ so that $(\bar{t}_0, \bar{t}_1, \bar{t}_2) = (3, 2, 3/2)$, $\bar{\nu} = 0$, $r = 1$, and $\nu_E = 0$. There are no edge states and we only show the energy spectrum along with the trajectory of $E(p)$ on the complex plane in Fig. 4.

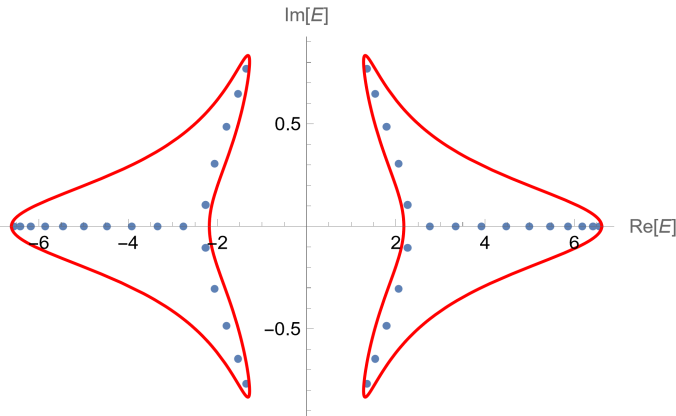


FIG. 4. The energy spectrum of the NH type 1 extended SSH model with 40 sites and the trajectory of $E(p)$ on the complex plane. Here, $(t_0^L, t_0^R, t_1^L, t_1^R, t_2^L, t_2^R) = (9/2, 2, 2, 2, 1, 9/4)$. Thus, $(\bar{t}_0, \bar{t}_1, \bar{t}_2) = (3, 2, 3/2)$ and it is in the trivial phase with $\bar{\nu} = 0$. Note that $\nu_E = 0$ and the energies of the eigenstates are encompassed by the trajectories of $E(p)$ on the complex plane.

Next, let's consider the case that $(t_0^L, t_0^R, t_1^L, t_1^R, t_2^L, t_2^R) = (1, 1, 10/3, 10/3, 3/4, 3)$ so that $(\bar{t}_0, \bar{t}_1, \bar{t}_2) = (1, 10/3, 3/2)$, $\bar{\nu} = 1$, $r = \sqrt{2}$, and $(\nu_E^L, \nu_E^R) = (1, -2)$. Here, we will continue to use the criteria we obtained in the QH case. We expect there would be one left and one right edge state. By taking the difference and sum of ψ_1 and ψ_2 , we indeed see the former one appears on the left boundary while the latter one is on the right. The energy spectrum, the trajectory of $E(p)$, and the wave functions of the edge states are shown in Fig. 5. Since the energies are now generally complex, the wave functions of the eigenstates would also be complex. Consequently, we only show the real part of a wave function, unless its magnitude is too small to be seen. In such cases, we would show the imaginary part instead. Note that all the energy eigenvalues, including those of the edge states, are enclosed by the trajectory to $E(p)$, which differs from the case that $\nu_E = 0$.

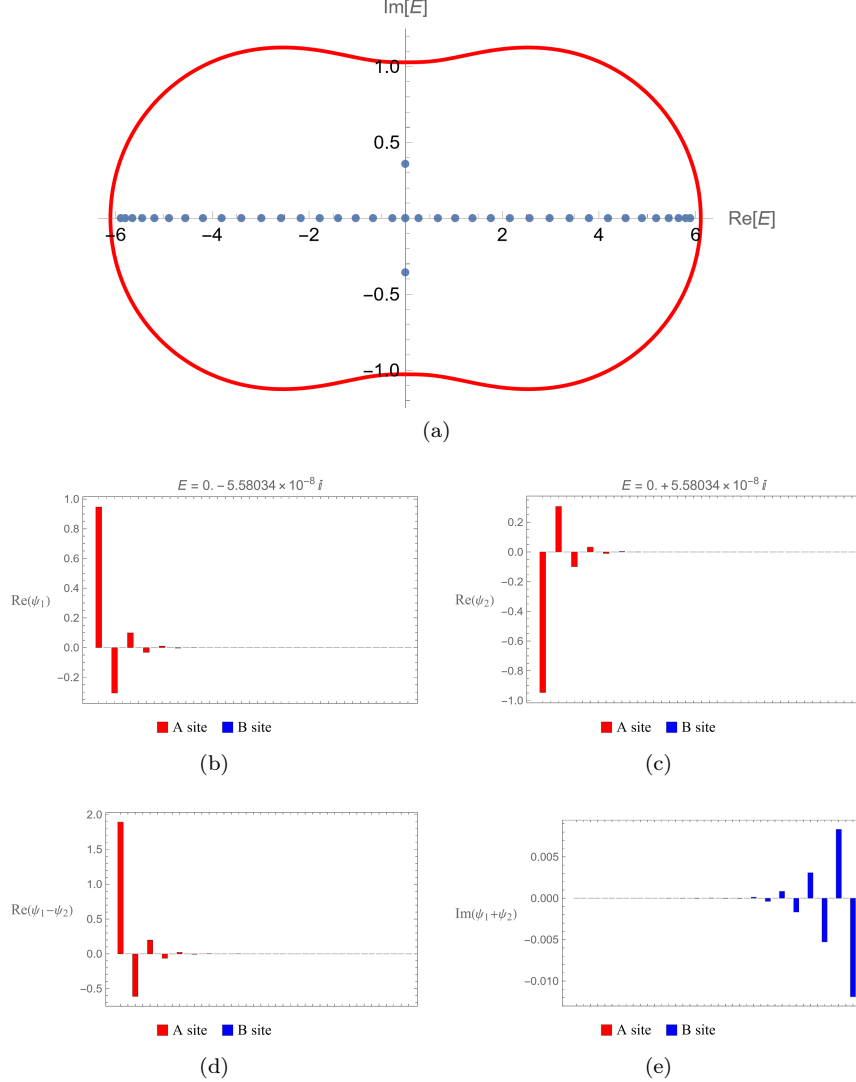


FIG. 5. (a) The energy spectrum of the NH type 1 extended SSH model with 40 sites, where $(t_0^L, t_0^R, t_1^L, t_1^R, t_2^L, t_2^R) = (1, 1, 10/3, 10/3, 3/4, 3)$. Thus, $(\bar{t}_0, \bar{t}_1, \bar{t}_2) = (1, 10/3, 3/2)$ and it is in the topological phase with $\bar{\nu} = 1$. Note that the energies of the two edge states ψ_1, ψ_2 are purely imaginary and approximately zero. They are also enclosed by the trajectory to $E(p)$. (b), (c) The wave functions of the two edge states in the system. (d), (e) The difference and sum of ψ_1 and ψ_2 . Note that $\psi_1 - \psi_2$ is a left edge state and $\psi_1 + \psi_2$ is a right edge state. This is consistent with the fact that $(\nu_E^L, \nu_E^R) = (1, -2)$.

Let's show one more example in which $(t_0^L, t_0^R, t_1^L, t_1^R, t_2^L, t_2^R) = (1, 1, 3, 3, 7/2, 4)$ so that $(\bar{t}_0, \bar{t}_1, \bar{t}_2) = (1, 3, \sqrt{14})$, $\bar{\nu} = 2$, $r = (8/7)^{1/4}$, and $(\nu_E^L, \nu_E^R) = (2, -2)$. The energies of the edge states are all complex with the same absolute value and form two complex conjugate pairs. As we mentioned, their locations all lie outside the trajectories of $E(p)$. By taking the difference and sum of (ψ_1, ψ_4) and (ψ_2, ψ_3) , we see there are two left and two right edge states. This is again consistent with the criteria obtained under the QHC. The energy spectrum, the trajectory of $E(p)$, and the

wave functions of the edge states are shown in Fig. 6.

Similarly, an analogous analysis may be conducted for the NH type 2 extended SSH model. Again, we leave the details in Appendix C to avoid repetition in the main text.

V. Conclusion and discussion

In this paper, we study the NH extended SSH models. Just like in the Hermitian case, there are two types of NH extended SSH models. We first focus on the quasi-Hermitian case, in which the hopping amplitudes obey a specific relation so that the system may be mapped to a corresponding Hermitian one and its energy spectrum is completely real. It is well-known that the conventional BBC may not be naively applied in an NH system. However, we may use the modified winding number $\bar{\nu}$ to classify the system and determine the total number of edge states on the boundaries analogous to the Hermitian case. Moreover, we show that the spectral winding numbers, (ν_E^L, ν_E^R) , may be used to classify the system further. It dictates how the edge states would be distributed over the left and right boundaries.

By analyzing the EOM and BCs of a finite chain of such a system, we are able to find the characteristic equation in terms of \bar{u}_1 and \bar{u}_2 , which in turn satisfy a linear relation implied by the secular equation. By solving numerically the characteristic and secular equations, we may find the energy spectrum of the system. The results are then compared to those obtained by numerically solving the matrix eigenvalue problem. They agree well with each other.

We then relax the QHC and consider general NH extended SSH models. Although we are still able to express the characteristic equation in terms of one single variable $\bar{u} = (\bar{s}_{12} + \bar{s}_{12}^{-1})/2$, the energy eigenvalues of such a system are complex in general. We continue to employ the classification in terms of $\bar{\nu}$ and (ν_E^L, ν_E^R) that we obtained under the QHC to check whether it is still applicable for general NH extended SSH models. For all the cases we considered, no inconsistency has been found. In principle, one may use the generalized BZ to calculate the modified winding number in general NH extended SSH models but we are not able to obtain an analytic expression at the moment. It is worth mentioning that similar to the Hermitian case, the two types of extended SSH models are related by a duality and may be mapped to each other by re-grouping the ‘‘atoms’’ in a unit cell.

It is known that non-Hermiticity also opens up the possibility that the Hamiltonian matrix becomes defective, and Jordan decomposition must be exploited to diagonalize such systems. As a result, generalized eigenvectors would appear. In the literature, this is referred to as an exceptional point in the parameter space of the hopping amplitudes. Finding the condition for exceptional points and their implications in NH systems remains an intriguing problem. Another interesting direction is to extend our analysis of 1D NH systems to 2D or higher dimensions. It is known that a relation between the 1D winding number and the 2D Chern number may be obtained if there is a certain symmetry in the system [56]. It would be interesting to carry out a similar study of NH systems to see whether such a relation still exists.

ACKNOWLEDGMENTS

The authors would like to thank Prof. Ming-Che Chang for stimulating discussions. J. S. Y. and H. C. K are partly supported by the Grants MOST-110-2112-M-003-008-MY3 and Grants MOST-110-2112-M-A49 -012 -MY2 of the Ministry of Science and Technology, Taiwan, respectively.

Appendix A: QH type 2 extended SSH models

The Hamiltonian of the NH type 2 extended SSH model with OBCs is given by:

$$H_{\text{ext}2} = \sum_{j=2}^{N-1} \left\{ \left(t_0^L A_j^\dagger + t_1^R A_{j+1}^\dagger + t_{-1}^L A_{j-1}^\dagger \right) B_j + \left(t_0^R A_j + t_1^L A_{j+1} + t_{-1}^R A_{j-1} \right) B_j^\dagger \right\} \quad (37)$$

$$+ \left(t_0^L A_1^\dagger + t_1^R A_2^\dagger \right) B_1 + \left(t_0^R A_1 + t_1^L A_2 \right) B_1^\dagger + \left(t_0^L A_N^\dagger + t_{-1}^L A_{N-1}^\dagger \right) B_N + \left(t_0^R A_N + t_{-1}^R A_{N-1} \right) B_N^\dagger.$$

Here, $t_{-1}^{L,R}$ are another type of third-nearest-neighbor left and right hopping amplitudes. It is again straightforward to achieve the EOM

$$EA_j - \left(t_0^L B_j + t_1^R B_{j-1} + t_{-1}^L B_{j+1} \right) = 0;$$

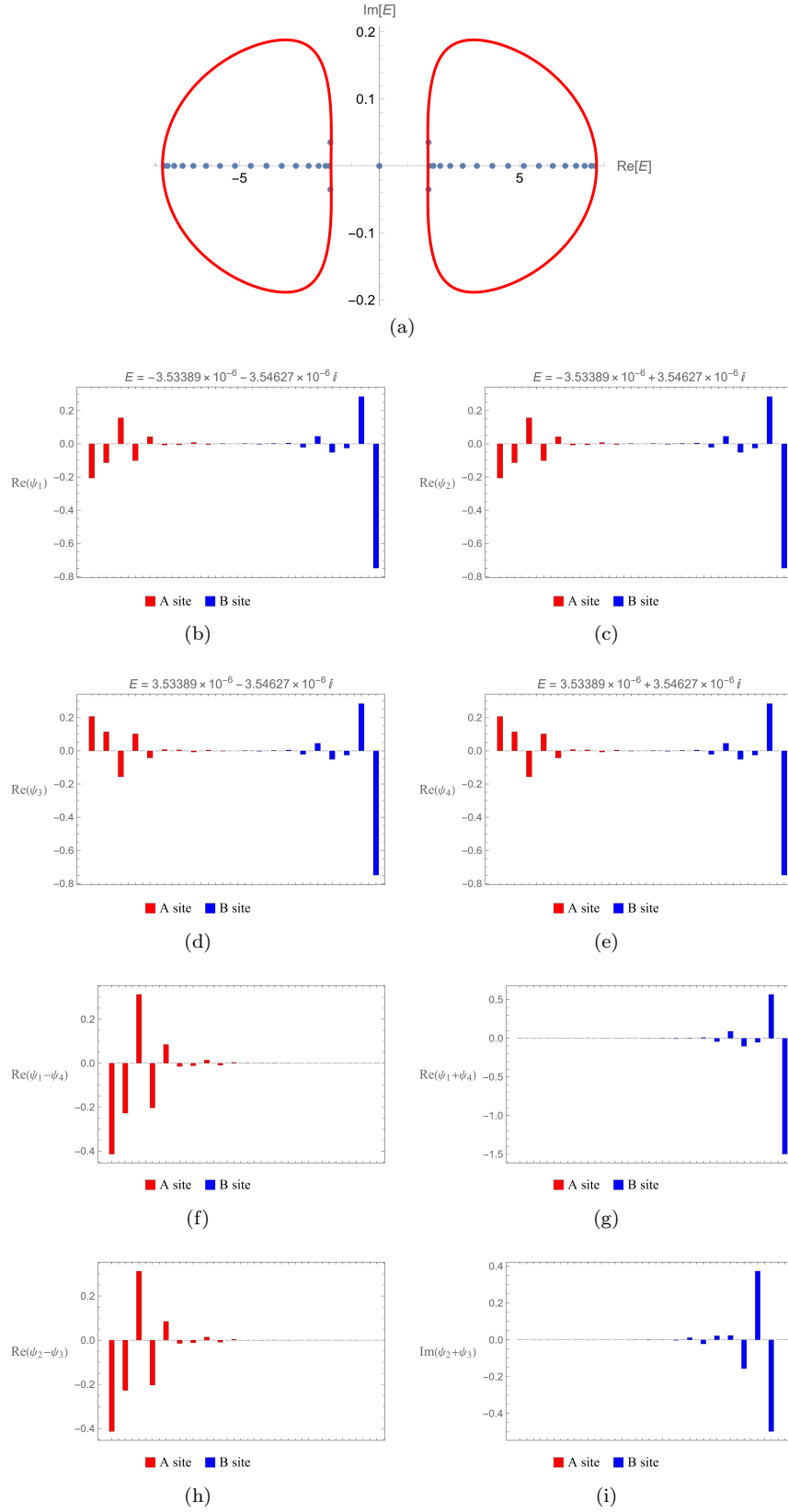


FIG. 6. (a) The energy spectrum of the NH type 1 extended SSH model with 40 sites, where $(t_0^L, t_0^R, t_1^L, t_1^R, t_2^L, t_2^R) = (1, 1, 3, 3, 7/2, 4)$. Thus, $(\bar{t}_0, \bar{t}_1, \bar{t}_2) = (1, 3, \sqrt{14})$ and it is in the topological phase with $\bar{\nu} = 2$. There are four edge states in total. (b), (c), (d), (e) The wave functions of the edge states $\psi_1, \psi_2, \psi_3, \psi_4$ in the system. They all have approximately zero energies. (f), (g) The difference and sum of (ψ_1, ψ_4) . (h), (i) The difference and sum of (ψ_2, ψ_3) . Note that there are both two edge states on the left and right boundaries, consistent with the fact that $\nu_E = 0$.

$$EB_j - (t_0^R A_j + t_1^L A_{j+1} + t_{-1}^R A_{j-1}) = 0, \quad \text{for } j = 2, \dots, N-1. \quad (38)$$

and BCs

$$\begin{aligned} B_0 &= A_0 = 0; \\ B_{N+1} &= A_{N+1} = 0. \end{aligned} \quad (39)$$

As pointed out in Ref. [56], type 1 and 2 extended SSH models are closely related. By renaming B_j and A_{j+1} as \tilde{A}_j and \tilde{B}_j , a bulk NH type 1 extended SSH model may be mapped to a bulk NH type 2 extended SSH model with the following correspondence:

$$\begin{aligned} (\tilde{t}_0^R, \tilde{t}_1^L, \tilde{t}_{-1}^R) &= (t_1^R, t_0^L, t_2^R); \\ (\tilde{t}_0^L, \tilde{t}_1^R, \tilde{t}_{-1}^L) &= (t_1^L, t_0^R, t_2^L). \end{aligned} \quad (40)$$

Substituting the above results into eq. (33), we have

$$E^2(p) = (\tilde{t}_0^R + \tilde{t}_1^L e^{ip} + \tilde{t}_{-1}^R e^{-ip}) (\tilde{t}_0^L + \tilde{t}_1^R e^{-ip} + \tilde{t}_{-1}^L e^{ip}). \quad (41)$$

Similarly, we have $\tilde{\nu}_E = \tilde{\nu}_E^L + \tilde{\nu}_E^R$, with $\tilde{\nu}_E^L$ and $\tilde{\nu}_E^R$ the spectral winding number corresponding to the former and latter factors, respectively. It is obvious that $\tilde{\nu}_E^R = \nu_E^L - 1$ and $\tilde{\nu}_E^L = \nu_E^R + 1$. Consequently, the winding numbers have the following relation:

$$\tilde{\nu}_E = \nu_E, \text{ and } \tilde{\bar{\nu}} = 1 - \bar{\nu}. \quad (42)$$

From now on, we will discard the tilde symbol to simplify expressions, as there is little chance of causing confusion. Following procedures similar to those in type1, we may have one single skin effect factor

$$r = [t_1^R t_{-1}^R / (t_1^L t_{-1}^L)]^{1/4}, \quad (43)$$

if the following QHC is satisfied

$$t_0^L = t_0^R \sqrt{t_1^R t_{-1}^L / (t_1^L t_{-1}^R)}. \quad (44)$$

This would translate into $(t_1 - \gamma_1/2) = (t_1 + \gamma_1/2) \sqrt{(t_2 + \gamma_2/2) / (t_2 - \gamma_2/2)}$ in the literature [43, 47, 48].

Similarly, the system may be mapped to a Hermitian type 2 extended SSH model with a real energy spectrum. In addition to \bar{t}_0, \bar{t}_1 , we introduce $\bar{t}_{-1} = \sqrt{t_{-1}^L t_{-1}^R}$, and the resultant characteristic equation may be expressed in terms of these parameters in the following form:

$$\begin{aligned} &\{U_{N+2}(\bar{u}_1)U_N(\bar{u}_2) - 2U_{N+1}(\bar{u}_1)U_{N+1}(\bar{u}_2) + U_N(\bar{u}_1)U_{N+2}(\bar{u}_2) + 2\} \\ &- \left[\frac{\bar{t}_1}{\bar{t}_{-1}} + \frac{\bar{t}_{-1}}{\bar{t}_1} \right] \{U_{N+1}(\bar{u}_1)U_{N-1}(\bar{u}_2) - 2U_N(\bar{u}_1)U_N(\bar{u}_2) + U_{N-1}(\bar{u}_1)U_{N+1}(\bar{u}_2) + 2\} \\ &+ \{U_N(\bar{u}_1)U_{N-2}(\bar{u}_2) - 2U_{N-1}(\bar{u}_1)U_{N-1}(\bar{u}_2) + U_{N-2}(\bar{u}_1)U_N(\bar{u}_2) + 2\} = 0. \end{aligned} \quad (45)$$

Similar to the type 1 case, the above characteristic equation is exactly the same as the one obtained in Ref. [56], if we identify the parameters $(\bar{t}_0, \bar{t}_1, \bar{t}_{-1})$ with (t_0, t_1, t_{-1}) .

Analogously, here we have

$$\begin{aligned} \bar{u}_1 + \bar{u}_2 &= -\bar{t}_0 (\bar{t}_1 + \bar{t}_{-1}) / (2\bar{t}_1 \bar{t}_{-1}), \\ E^2 &= \bar{t}_0^2 + \bar{t}_1^2 + \bar{t}_{-1}^2 + 2\bar{t}_1 \bar{t}_{-1} (1 + 2\bar{u}_1 \bar{u}_2). \end{aligned} \quad (46)$$

Again, they are symmetric with respect to \bar{u}_1 and \bar{u}_2 and we may remove the redundancy in the solutions of \bar{u}_1 and \bar{u}_2 by requiring $\bar{u}_1 > \bar{u}_2$.

Similar to the type 1 case, we may use the modified winding number $\bar{\nu}$ to classify such a system into three different phases:

- 1) $\bar{t}_1 + \bar{t}_{-1} > \bar{t}_0$, and $\bar{t}_1 > \bar{t}_{-1}$: The system is in the topological phase with $\bar{\nu} = 1$ and two edge states on the boundaries.
- 2) $\bar{t}_1 + \bar{t}_{-1} < \bar{t}_0$: The system is in the trivial phase with $\bar{\nu} = 0$ and no edge states.

- 3) $\bar{t}_1 + \bar{t}_{-1} > \bar{t}_0$, and $\bar{t}_1 < \bar{t}_{-1}$: The system is in the topological phase with $\bar{\nu} = -1$ and two edge states on the boundaries.

Just like in the type 1 case, the edge states are generally not evenly distributed over the left and right boundaries due to the skin effect. Similarly, we may use ν_E^L and ν_E^R to determine where they would appear:

- 1) $\bar{\nu} = 1$ or $\bar{\nu} = -1$:

- i) $(\nu_E^L, \nu_E^R) = (1, 1), (0, 1), \boxed{(1, 0)}$. Both edge states are on the left boundary.
- ii) $(\nu_E^L, \nu_E^R) = \boxed{(1, 0)}, (1, -1), (0, 0), (-1, 1), \boxed{(0, -1)}$. One edge state is on the left boundary and one on the right.
- iii) $(\nu_E^L, \nu_E^R) = \boxed{(0, -1)}, (-1, 0), (-1, -1)$. Both edge states are on the right boundary.

- 2) $\bar{\nu} = 0$: $\nu_E = 2, 1, 0, -1, 2$. No edge state.

Note that we put a box around $(1, 0)$ and $(0, -1)$ to indicate that there is an ambiguity in determining the locations of the edge states when (ν_E^L, ν_E^R) equal to these values.

For demonstration, we consider the case $(t_0^L, t_0^R, t_1^L, t_1^R, t_{-1}^L, t_{-1}^R) = (4, 4, 1, 1/4, 10, 5/2)$ so that $(\bar{t}_0, \bar{t}_1, \bar{t}_{-1}) = (4, 1/2, 5)$, $\bar{\nu} = -1$ and $r = 1/2$. There are two edge states, which we call ψ_1 and ψ_2 . Since $(\nu_E^L, \nu_E^R) = (0, 1)$, both edge states show up on the left boundary due to the skin effect. Again, this may be seen explicitly by taking the difference and sum of ψ_1 and ψ_2 . In particular, $\psi_1 + \psi_2$ is non-vanishing on the B sites only. We show the results in Fig. 7.

We would like to point out that although the $\bar{\nu} = 1$ and $\bar{\nu} = -1$ cases both have two edge states in total, we may still tell the difference between them by looking at the wave functions of the edge states. In particular, if we compare the results of the case that $(t_0^L, t_0^R, t_1^L, t_1^R, t_{-1}^L, t_{-1}^R) = (4, 4, 10, 5/2, 1, 1/4)$ so that $(\bar{t}_0, \bar{t}_1, \bar{t}_{-1}) = (4, 5, 1/2)$, $\bar{\nu} = 1$, $(\nu_E^L, \nu_E^R) = (1, 0)$ and $r = 1/2$ to those of the previous case, we will see that now both edge states are mainly on the A sites instead of B sites.

Appendix B: QH extended SSH models with an odd number of sites

In the type 1 case, if there are $2N + 1$ sites so that the chain ends with A_{N+1} rather than B_N on the right boundary, then the corresponding BCs on the right becomes

$$B_{N+1} = A_{N+2} = 0. \quad (47)$$

Following similar steps carried out previously, we may again find the corresponding characteristic equation for \bar{s} :

$$\begin{aligned} & \{U_{N+2}(\bar{u}_1)U_N(\bar{u}_2) - 2U_{N+1}(\bar{u}_1)U_{N+1}(\bar{u}_2) + U_N(\bar{u}_1)U_{N+2}(\bar{u}_2) + 2\} \\ & - (\bar{t}_2/\bar{t}_0) \{U_{N+1}(\bar{u}_1)U_{N-1}(\bar{u}_2) - 2U_N(\bar{u}_1)U_N(\bar{u}_2) + U_{N-1}(\bar{u}_1)U_{N+1}(\bar{u}_2) + 2\} = 0. \end{aligned} \quad (48)$$

Since the unit cell defined by the two sites by the right boundary differs from the one by the left boundary, the corresponding winding numbers would also be different. From eq. (40), we see the right boundary of the type 1 extended SSH model would be mapped to that of the type 2 extended SSH model. Hence, from the unit cell by the right boundary we have $\tilde{\nu}_E^R = \nu_E^L - 1$ and $\tilde{\nu}_E^L = \nu_E^R + 1$ and $\tilde{\nu} = 1 - \bar{\nu}$.

In Fig. 8, we show the energy spectrum and wave functions of the edge states for the case that all the parameters remain the same as those considered in Fig. 2, but there are now 41 sites in the system. Using the unit cell by the left boundary, we have $\bar{\nu} = 2$. In contrast, using the unit cell by the right boundary, we have $\tilde{\nu} = -1$. Hence, there are three edge states, which we call ψ_1, ψ_2 , and ψ_3 . Moreover, since $(\nu_E^L, \nu_E^R) = (2, -1)$ the left boundary contributes two left edge states and $(\tilde{\nu}_E^L, \tilde{\nu}_E^R) = (0, 1)$ so the right boundary contributes one left edge states. This is a reflection of the skin effect. Among them, ψ_1 and ψ_3 have almost zero energies and form a chiral conjugate pair. In contrast, ψ_2 is an exact zero energy state protected by the chiral symmetry and it is non-vanishing only on the A sites [57]. Taking the sum of ψ_1 and ψ_3 , we however achieve a wave function that is non-vanishing only on the B sites.

For the case of the NH type 2 extended SSH model with $2N + 1$ sites, we may obtain the corresponding characteristic equation by making the following substitution $(\bar{t}_0, \bar{t}_1, \bar{t}_2) \rightarrow (\bar{t}_1, \bar{t}_0, \bar{t}_{-1})$ in eq. (48). The reason is that when there are an odd number of sites in the system, the right boundary of a type 2 system is equivalent to that of a type 1 system as discussed in Appendix A. Therefore, it would be nothing but a space inversion of the system that we just considered.

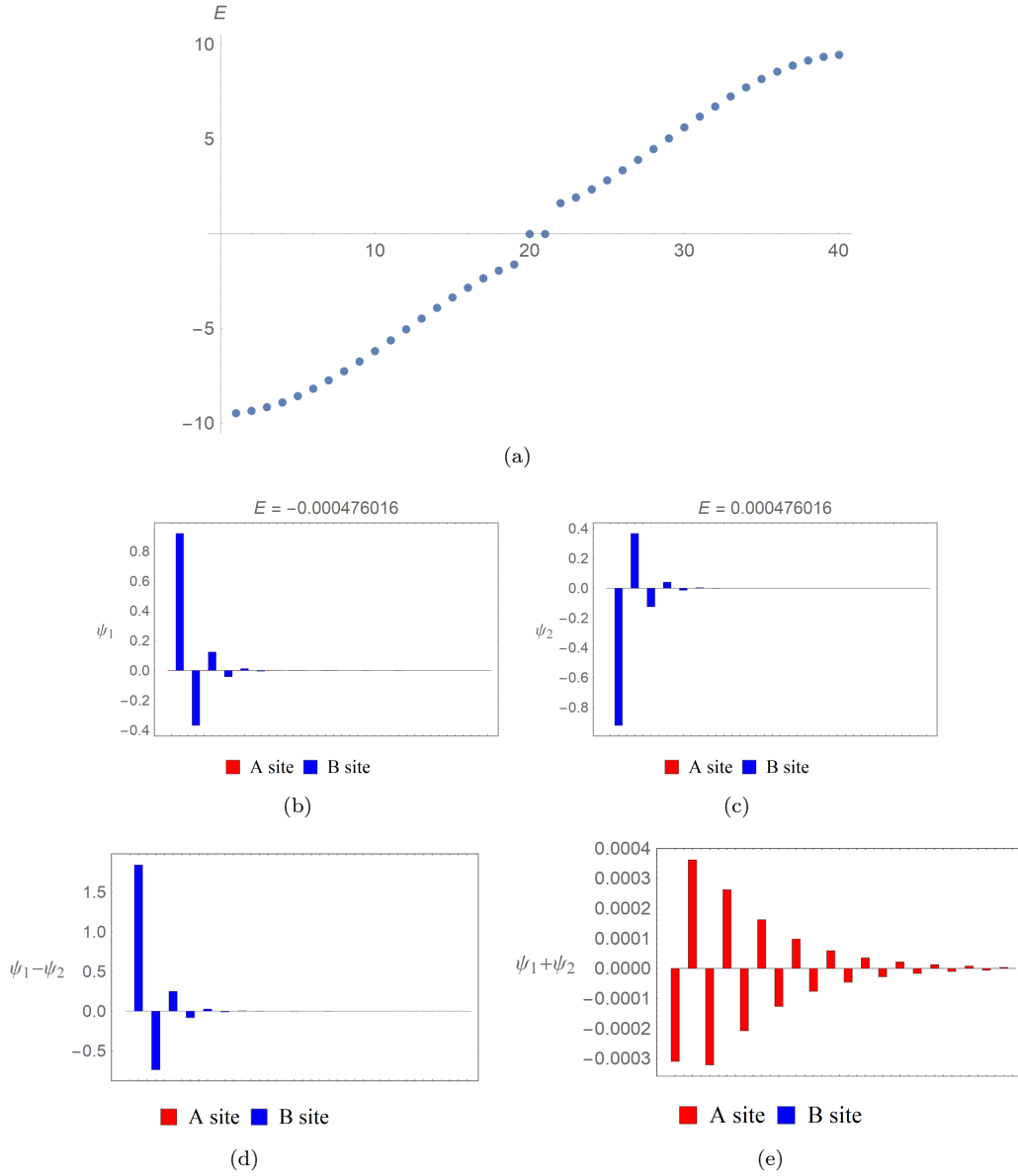


FIG. 7. (a) The energy spectrum of the NH type 2 extended SSH model, where $(t_0^L, t_0^R, t_1^L, t_1^R, t_{-1}^L, t_{-1}^R) = (4, 4, 1, 1/4, 10, 5/2)$. As a result, $(\bar{t}_0, \bar{t}_1, \bar{t}_{-1}) = (4, 1/2, 5)$ and the system is in the topological phase $\bar{\nu} = -1$. The energies of the two edge states ψ_1, ψ_2 are both approximately zero. (b), (c) The wave functions of the two edge states in the system. (d), (e) The difference and sum of ψ_1 and ψ_2 . Note that both left edge states appear on the left boundary as $(\nu_E^L, \nu_E^R) = (0, 1)$.

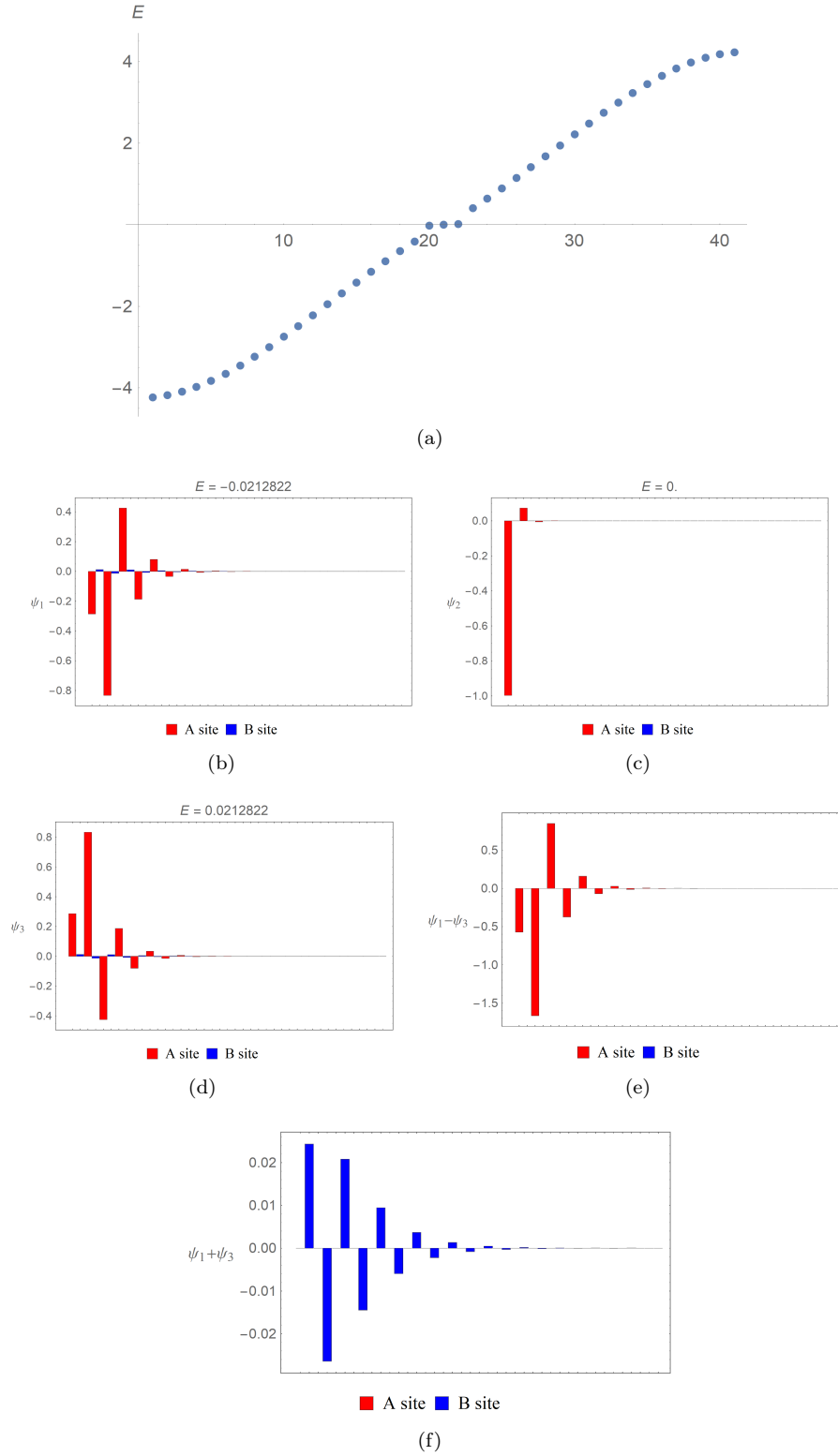


FIG. 8. (a) The energy spectrum of the NH type 1 extended SSH model with 41 sites. The values of the parameters remain exactly the same as those in Fig. 2 and thus $\bar{\nu} = 2$. However, since the number of sites in the system is odd, the modified winding number corresponding to the unit cell by the right boundary is now $\bar{\nu}_R = 1 - \bar{\nu}_L = -1$. (b), (c), (d) Wave functions of the edge states ψ_1, ψ_2, ψ_3 . The energies of the edge states ψ_1 and ψ_3 are approximately zero, while ψ_2 is a state with exact zero energy. Note that they are all left edge states. (e), (f) The difference and sum of ψ_1 and ψ_3 . Note that $\psi_1 + \psi_3$ is non-vanishing on the B sites only.

Appendix C: General NH type 2 extended SSH model

Similarly for a general NH type 2 extended SSH model, the characteristic equation may be expressed in terms of s_{12} , s_{34} , u_{12} , and u_{34} :

$$\begin{aligned}
& \left\{ -(t_{-1}^L)^2 s_{12}^N s_{34}^{N+2} U_N(u_{34}) U_N(u_{12}) + t_{-1}^L s_{12}^{N-1} s_{34}^{N+1} U_{N+1}(u_{34}) [t_{-1}^L s_{12}^2 U_{N-1}(u_{12}) + t_1^R U_{N+1}(u_{12})] \right. \\
& - t_1^R t_{-1}^L s_{12}^N s_{34}^N U_{N+2}(u_{34}) U_N(u_{12}) + t_{-1}^L s_{12}^{N-1} s_{34}^{N+1} U_{N-1}(u_{34}) [t_{-1}^L s_{12}^2 U_{N+1}(u_{12}) + t_1^R s_{12} U_{N-1}(u_{12})] \\
& - s_{12}^{N-2} s_{34}^N U_N(u_{34}) [(t_0^L)^2 s_{12}^4 U_N(u_{12}) + t_1^R t_{-1}^L s_{12}^2 U_{N+2}(u_{12}) + t_1^R t_{-1}^L s_{12}^2 U_{N-2}(u_{12}) + (t_1^R)^2 U_N(u_{12})] \\
& + t_1^R s_{12}^{N-1} s_{34}^{N-1} U_{N+1}(u_{34}) [t_{-1}^L s_{12}^2 U_{N+1}(u_{12}) + t_1^R U_{N-1}(u_{12})] - (t_1^R)^2 s_{12}^N s_{34}^{N-2} U_N(u_{34}) U_N(u_{12}) \\
& \left. - t_1^R t_{-1}^L s_{12}^N s_{34}^N U_{N-2}(u_{34}) U_N(u_{12}) + t_1^R s_{12}^{N-1} s_{34}^{N-1} U_{N-1}(u_{34}) [t_{-1}^L s_{12}^2 U_{N-1}(u_{12}) + t_1^R U_{N+1}(u_{12})] \right\} \\
& + (t_1^R - t_{-1}^L s_{12}^2)(t_1^R - t_{-1}^L s_{34}^2) [s_{12}^{-4} s_{34}^{2N} + s_{12}^{2N} s_{34}^{-4}] = 0. \tag{49}
\end{aligned}$$

Again, we may express u_{12} , u_{34} in terms of s_{12} , s_{34} :

$$\begin{aligned}
u_{12} &= \frac{s_{12} s_{34} \{ t_1^L t_{-1}^L (t_0^R t_1^R + t_0^L t_{-1}^R) s_{34} - t_1^R t_{-1}^R (t_0^L t_1^L + t_0^R t_{-1}^L) s_{34}^{-1} \}}{2 t_1^L t_1^R t_{-1}^L t_{-1}^R (s_{12}^2 - s_{34}^2)}, \\
u_{34} &= \frac{-s_{12} s_{34} \{ t_1^L t_{-1}^L (t_0^R t_1^R + t_0^L t_{-1}^R) s_{12} - t_1^R t_{-1}^R (t_0^L t_1^L + t_0^R t_{-1}^L) s_{12}^{-1} \}}{2 t_1^L t_1^R t_{-1}^L t_{-1}^R (s_{12}^2 - s_{34}^2)}. \tag{50}
\end{aligned}$$

By making use of eq. (50), the characteristic equation may be written in terms of s_{12} and s_{34} . Similarly, the characteristic equation may be expressed in terms of one single variable $\bar{u} = (\bar{s}_{12} + \bar{s}_{12}^{-1})/2$. Again, the resultant characteristic equation is a polynomial in \bar{u} of degree $3N$ after simplification.

As an example, let's choose the parameters to be $(t_0^L, t_0^R, t_1^L, t_1^R, t_{-1}^L, t_{-1}^R) = (2, 2, 9/2, 2, 1, 9/4)$ so that $(\bar{t}_0, \bar{t}_1, \bar{t}_{-1}) = (2, 3, 3/2)$, $\bar{\nu} = 1$, $r = 1$, and $(\nu_E^L, \nu_E^R) = (1, -1)$. As expected, there are two edge states with one on the left and the other on the right boundary. We show the energy spectrum along with the trajectory of $E(p)$ on the complex plane and the wave functions of the edge states in Fig. 9. It is obvious that the NH type 2 extended SSH model we consider here is dual to the NH type 1 extended SSH model shown in Fig. 4 through the mapping given in eq. (40). In particular, Fig. 9a and Fig. 4 are almost identical except for the existence of edge states.

Let's consider another example with $(t_0^L, t_0^R, t_1^L, t_1^R, t_{-1}^L, t_{-1}^R) = (3, 3, 1, 1, 7/2, 4)$ so that $(\bar{t}_0, \bar{t}_1, \bar{t}_{-1}) = (3, 1, \sqrt{14})$, $\bar{\nu} = -1$, $r = (8/7)^{1/4}$, and $(\nu_E^L, \nu_E^R) = (-1, 1)$. Again, there is one left and one right edge state. The energy spectrum along with the trajectory of $E(p)$ on the complex plane and the wave functions of the edge states are shown in Fig. 10. The NH type 2 extended SSH model we consider here is dual to the NH type 1 extended SSH model, shown in Fig. 6. Likewise, the energy spectra and the trajectories of $E(p)$ are both similar.

We also check the four cases considered in Ref. [47], where $(t_0^L, t_0^R, t_1^L, t_1^R, t_{-1}^L, t_{-1}^R) = (1.1+2/3, 1.1-2/3, 1, 1, 1/5, 1/5)$, $(-1.1+2/3, -1.1-2/3, 1, 1, 1/5, 1/5)$, $(0.3, 0.3, 1.1+2/3, 1.1-2/3, 1/5, 1/5)$, and $(0.3, 0.3, 1.1-2/3, 1.1+2/3, 1/5, 1/5)$. The corresponding $\bar{\nu}$ are all 1, and $(\nu_E^L, \nu_E^R) = (1, 0)$, $(0, -1)$, $(1, -1)$ and $(1, -1)$, respectively. Again, the total number of edge states and their locations are consistent with the criteria we obtain in the QH case.

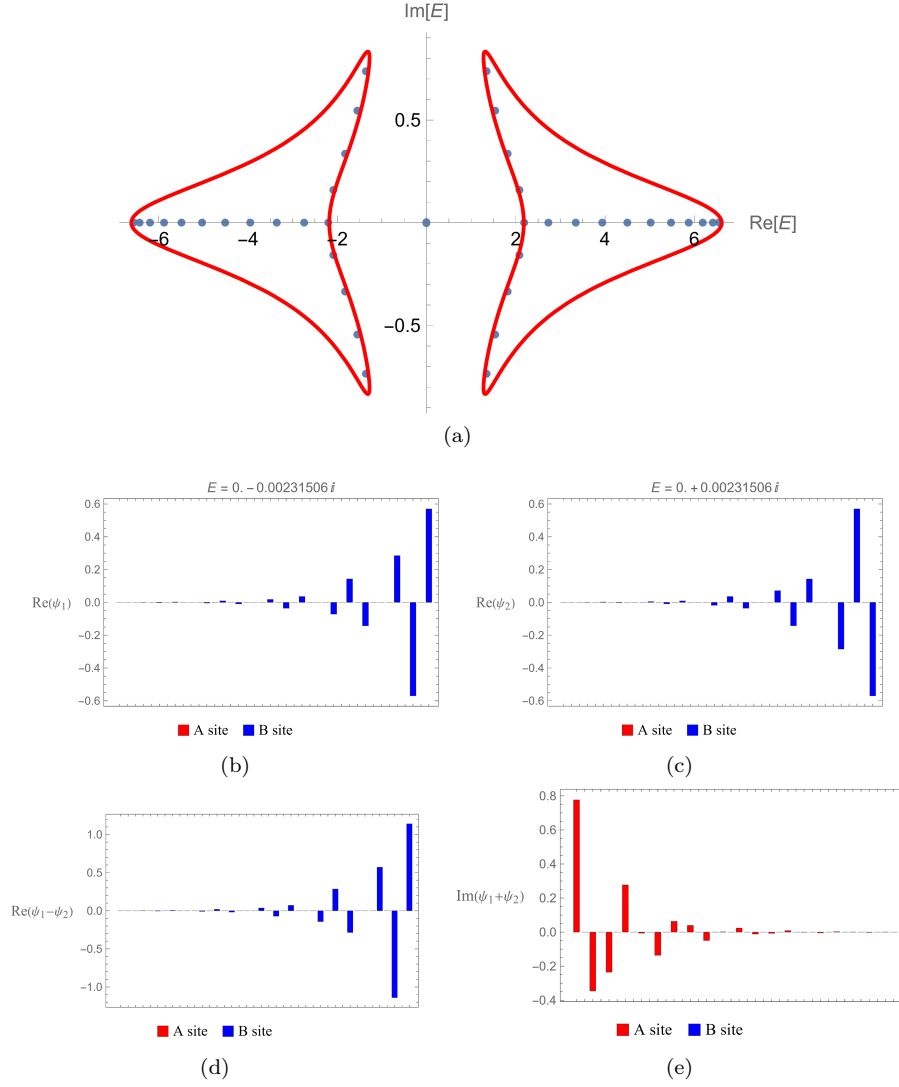


FIG. 9. The energy spectrum of the NH type 2 extended SSH model with 40 sites and the trajectory of $E(p)$ on the complex plane. Here, $(t_0^L, t_0^R, t_1^L, t_1^R, t_{-1}^L, t_{-1}^R) = (2, 2, 9/2, 2, 1, 9/4)$. Thus, $(\bar{t}_0, \bar{t}_1, \bar{t}_2) = (2, 3, 3/2)$ and it is in the topological phase with $\bar{\nu} = 1$. Note that there are one left and one right edge states, which is consistent with the fact that $(\nu_E^L, \nu_E^R) = (1, -1)$. As mentioned, the energies of the eigenstates except for the edge states are encompassed by the trajectories of $E(p)$ on the complex plane.

-
- [1] M. Z. Hasan and C. L. Kane, "Topological insulators," *Rev. Mod. Phys.*, **82**, (2010).
[2] X.-L. Qi and S.-C. Zhang, "Topological insulators and superconductors," *Rev. Mod. Phys.*, **83**, (2011).
[3] A. P. Schnyder, S. Ryu, A. Furusaki, and A. W. W. Ludwig, "Classification of topological insulators and superconductors in three spatial dimensions," *Phys. Rev. B* **78**, 195125 (2008).
[4] A. Kitaev, "Periodic table for topological insulators and superconductors," *AIP Conf. Proc.* 1134, 22 (2009).
[5] A. P. Schnyder, S. Ryu, A. Furusaki, and A. W. W. Ludwig, "Classification of Topological Insulators and Superconductors," *AIP Conf. Proc.* 1134, 10 (2009).
[6] W. P. Su, J. R. Schrieffer, and A. J. Heeger, "Solitons in Polyacetylene," *Phys. Rev. Lett.* **42**, 1698, (1979).
[7] M. Kiczynski *et al.*, "Engineering topological states in atom-based semiconductor quantum dots," *Nature* 606, 694 (2022).
[8] J. Zak, "Berry's phase for energy bands in solids," *Phys. Rev. Lett.*, **62**, 2747, (1989).
[9] M. V. Berry, "Quantal phase factors accompanying adiabatic changes," *Proc. R. Soc. Lond. A.* **392**, 45, (1984).
[10] M. Atala *et al.*, "Direct Measurement of the Zak phase in Topological Bloch Bands," *Nature Phys.* 9, 795–800 (2013).
[11] J. K. Asboth, L. Oroszlany, and A. Palyi, "A Short Course on Topological Insulators," arXiv:1509.02295.
[12] D.J. Thouless, "Quantization of particle transport," *Phys. Rev. B* **27**, 6083–6087 (1983)

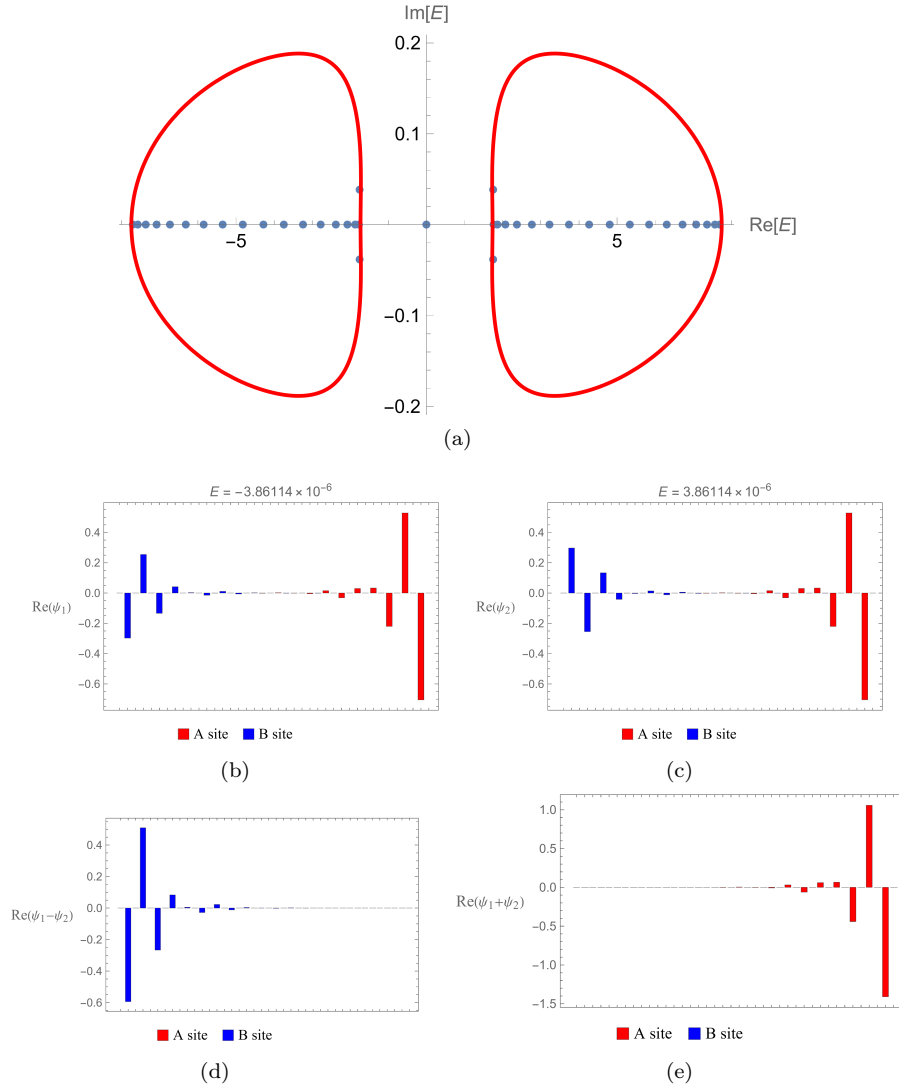


FIG. 10. The energy spectrum of the NH type 2 extended SSH model with 40 sites and the trajectory of $E(p)$ on the complex plane. Here, $(t_0^L, t_0^R, t_1^L, t_1^R, t_{-1}^L, t_{-1}^R) = (3, 3, 1, 1, 7/2, 4)$. Thus, $(\bar{t}_0, \bar{t}_1, \bar{t}_2) = (3, 1, \sqrt{14})$ and it is in the topological phase with $\bar{\nu} = -1$. Note that $(\nu_E^L, \nu_E^R) = (-1, 1)$ and the energies of the eigenstates except for the edge states are encompassed by the trajectories of $E(p)$ on the complex plane.

- [13] R. D. King-Smith and D. Vanderbilt, "Theory of polarization of crystalline solids," *Phys. Rev. B* **47**, 1651(R) (1993).
- [14] D. Vanderbilt and R. D. King-Smith, "Electric polarization as a bulk quantity and its relation to surface charge," *Phys. Rev. B* **48**, 4442 (1993).
- [15] V. M. Martinez Alvarez and M. D. Coutinho-Filho, "Edge states in trimer lattices," *Phys. Rev. A* **99**, 013833 (2019).
- [16] Y. Zhang, B. Ren, Y. Li, and F. Ye, "Topological states in the super-SSH model," *Optics Express* **29**, 42827, (2021).
- [17] Chen-Shen Lee, Iao-Fai Io, and Hsien-chung Kao, "Winding number and Zak phase in multi-band SSH models," *Chinese Journal of Physics*, **78**, 96 (2022).
- [18] R. Leone, "The geometry of (non)-Abelian adiabatic pumping," *J. Phys. A: Math. Theor.* **44**, 295301 (2011).
- [19] F. Wilczek and A. Zee, "Appearance of Gauge Structure in Simple Dynamical Systems," *Phys. Rev. Lett.* **52**, 2111 (1984).
- [20] K. N. Kudin, R. Car, and R. Resta, "Berry phase approach to longitudinal dipole moments of infinite chains in electronic-structure methods with local basis sets," *J. Chem. Phys.* **126**, 234101 (2007).
- [21] J.-W. Rhim, J. Behrends, and J. H. Bardarson, "Bulk-boundary correspondence from the intercellular Zak phase," *Phys. Rev. B* **95**, 035421 (2017).
- [22] E. J. Bergholtz, J. C. Budich, and F. K. Kunst, "Exceptional topology of non-Hermitian systems," *Rev. Mod. Phys.* **93**, 015005 (2021).
- [23] N. Okuma and M. Sato, "Non-Hermitian Topological Phenomena: A Review," *Annual Review of Condensed Matter Physics* **14**, 83 (2022).
- [24] Y. Ashida, Z. Gong, and M. Ueda, "Non-Hermitian physics," *Advances in Physics* **69**, 249 (2020)

- [25] K. Ding, C. Fang, and G. Ma, "Non-Hermitian Topology and Exceptional-Point Geometries," *Nature Reviews Physics* **4**, 745 (2022).
- [26] C. Poli *et al.*, "Selective enhancement of topologically induced interface states in a dielectric resonator chain," *Nat. Commun.* **6**, 6710 (2015).
- [27] J. M. Zeuner *et al.*, "Observation of a Topological Transition in the Bulk of a Non-Hermitian System," *Phys. Rev. Lett.* **115**, 040402 (2015).
- [28] W. Chen *et al.*, "Exceptional points enhance sensing in an optical microcavity," *Nature (London)* **548**, 192 (2017).
- [29] H. Hodaei *et al.*, "Enhanced sensitivity at higher-order exceptional points," *Nature (London)* **548**, 187 (2017).
- [30] S. Weimann *et al.*, "Topologically protected bound states in photonic parity-timesymmetric crystals," *Nat. Mater.* **16**, 433 (2017).
- [31] M. A. Bandres *et al.*, "Topological insulator laser: Experiments," *Science* **359**, eaar4005 (2018).
- [32] H. Zhou *et al.*, "Observation of bulk Fermi arc and polarization half charge from paired exceptional points," *Science* **359**, 1009–1012 (2018).
- [33] A. Cerjan *et al.*, "Experimental realization of a Weyl exceptional ring," *Nat. Photonics* **13**, 623–628 (2019).
- [34] T. Helbig *et al.*, "Generalized bulk-boundary correspondence in non-Hermitian topoelectrical circuits," *Nat. Phys.* **16**, 747–750 (2020).
- [35] L. Xiao *et al.*, "Non-Hermitian bulk-boundary correspondence in quantum dynamics," *Nature Physics* **16**, 761 (2020).
- [36] Hatano, N., and D. R. Nelson, "Localization Transitions in Non-Hermitian Quantum Mechanics," *Phys. Rev. Lett.* **77**, 570 (1996).
- [37] Z. Gong *et al.*, "Topological Phases of Non-Hermitian Systems," *Phys. Rev. X* **8**, 031079 (2018).
- [38] H. Shen, B. Zhen, and L. Fu, "Topological Band Theory for Non-Hermitian Hamiltonians," *Phys. Rev. Lett.* **120**, 146402 (2018).
- [39] K. Kawabata, N. Okuma, and M. Sato, "Non-Bloch band theory of non-Hermitian Hamiltonians in the symplectic class," *Phys. Rev. B* **101**, 195147 (2020).
- [40] F. K. Kunst, E. Edvardsson, J. C. Budich, and E. J. Bergholtz, "Biorthogonal Bulk-Boundary Correspondence in Non-Hermitian Systems," *Phys. Rev. Lett.* **121**, 026808 (2018).
- [41] Martinez Alvarez, V. M., J. E. Barrios Vargas, and L. E. F. Foa Torres, "Non-Hermitian robust edge states in one dimension: Anomalous localization and eigenspace condensation at exceptional points," *Phys. Rev. B* **97**, 121401 (2018).
- [42] Xiong, Y., "Why does bulk boundary correspondence fail in some non-Hermitian topological models," *J. Phys. Commun.* **2**, 035043 (2018).
- [43] S. Yao and Z. Wang, "Edge States and Topological Invariants of Non-Hermitian Systems," *Phys. Rev. Lett.* **121**, 086803 (2018).
- [44] T. E. Lee, "Anomalous Edge State in a Non-Hermitian Lattice," *Phys. Rev. Lett.* **116**, 133903 (2016).
- [45] S. Yao, F. Song, and Z. Wang, "Non-Hermitian Chern Bands," *Phys. Rev. Lett.* **121**, 136802 (2018).
- [46] Deng, T. S., and W. Yi, "Non-Bloch topological invariants in a non-Hermitian domain wall system," *Phys. Rev. B* **100**, 035102 (2019).
- [47] K. Yokomizo, and S. Murakami, "Non-Bloch Band Theory of Non-Hermitian Systems," *Phys. Rev. Lett.* **123**, 066404 (2019).
- [48] Z. Yang, K. Zhang, C. Fang, and J. Hu, "Non-Hermitian Bulk-Boundary Correspondence and Auxiliary Generalized Brillouin Zone Theory," *Phys. Rev. Lett.* **125**, 226402 (2020).
- [49] Edvardsson, E., F. K. Kunst, and E. J. Bergholtz, "Non-Hermitian extensions of higher-order topological phases and their biorthogonal bulk-boundary correspondence," *Phys. Rev. B* **99**, 081302 (2019).
- [50] Edvardsson, E., F. K. Kunst, T. Yoshida, and E. J. Bergholtz, "Phase transitions and generalized biorthogonal polarization in non-Hermitian systems," *Phys. Rev. Research* **2**, 043046 (2020).
- [51] S. Yao, F. Song, and Z. Wang, "Non-Hermitian Chern Bands," *Phys. Rev. Lett.* **121**, 136802 (2018).
- [52] A. Mostafazadeh, "Pseudo-Hermiticity versus PT symmetry: The necessary condition for the reality of the spectrum of a non-Hermitian Hamiltonian," *J. Math. Phys. (N.Y.)* **43**, 205–214 (2002).
- [53] C. Yin *et al.*, "Geometrical meaning of winding number and its characterization of topological phases in one-dimensional chiral non-Hermitian systems," *Phys. Rev. A* **97**, 052115 (2018).
- [54] R. Wakatsuki, M. Ezawa, and N. Nagaosa, *Phys. Rev. B* **89**, 174514 (2014).
- [55] Ken-Ichiro Imura and Yositate Takane, "Generalized bulk-edge correspondence for non-Hermitian topological systems," *Phys. Rev. B* **100**, 165430, (2019).
- [56] Han-Ting Chen, Chia-Hsun Chang, and Hsien-chung Kao, "Connection between the winding number and the Chern number," *Chinese Journal of Physics*, **72**, 50-68, (2021).
- [57] H. C. Kao, "Chiral zero modes in superconducting nanowires with Dresselhaus spin-orbit coupling," *Phys. Rev. B* **90**, 245435 (2014).